heritage

MDPI

Article

An Invisible Archive: Multi-Analytical Investigation of Medieval Manuscript Production in Benevento

Francesco Di Concilio [1,2], Annalaura Casanova Municchia [3,*], Maria Catrambone [3], Alessandra Chirivì [4], Myriam Fiore [1,5], Marco Ferretti [3], Margherita Giugni [1,2], Mario Iadanza [6], Costanza Miliani [1] and Gemma Teresa Colesanti [1]

1 Institute of Heritage Science, National Research Council (CNR-ISPC), 80134 Naples, NA, Italy; francescodiconcilio@cnr.it (F.D.C.); myriamfiore@cnr.it (M.F.); margheritagiugni@cnr.it (M.G.); costanza.miliani@cnr.it (C.M.); gemmateresa.colesanti@cnr.it (G.T.C.)
2 Department of Antiquities, Faculty of Humanities, Sapienza University of Rome, Piazzale Aldo Moro 5, 00185 Rome, RM, Italy
3 Institute of Heritage Science, National Research Council (CNR-ISPC), 00010 Montelibretti, RM, Italy; maria.catrambone@cnr.it (M.C.); marco.ferretti@cnr.it (M.F.)
4 Institute of Heritage Science, National Research Council (CNR-ISPC), 73100 Lecce, LE, Italy; alessandra.chirivi@cnr.it
5 Department of Chemical Sciences, University of Naples Federico II, Complesso Universitario di Monte S. Angelo, Via Cinthia 21, 80126 Naples, NA, Italy
6 Ufficio per i Beni Culturali e l'Arte Sacra dell'Arcidiocesi di Benevento, 82100 Benevento, BN, Italy
* Correspondence: annalaura.casanovamunicchia@cnr.it; Tel.: +39-06-9067-2725

Abstract

The twelfth-century Beneventan manuscripts of the Cathedral Chapter Library of Benevento constitute a largely understudied corpus of medieval illumination, whose material composition has not yet been investigated. This paper presents an *in situ* non-invasive multi-analytical investigation of three of these codices: Ms. 7 and Ms. 17 (Sanctorale), and Ms. 19 (Missal–Breviary) assigned to two different production environments, through a workflow combining elemental/molecular spectroscopy with point-based and Vis-NIR hyperspectral imaging and high-resolution microscopy. The study examines pigments, binders, and inks, across the three manuscripts, with the aim of establishing an exploratory research protocol that combines autoptic observations and diagnostic analyses to characterising and comparing manuscript production environments. The principal pigments identified across the three manuscripts are cinnabar, natural ultramarine (lapis lazuli), a copper-based green, and lead white, with iron-gall ink consistently present for text writing. Notable differences between the two production environments include the use of orpiment versus an unidentified organic lake for yellow, and the presence of minium, a red–purple lake, and gold exclusively in Ms. 19. A particularly significant finding is the use of iron gall ink, employed across all three manuscripts as a writing medium and as a pigment for modulating tonal values. Moreover, a brown ink was identified in preparatory underdrawings and decorative details, but its composition remains undetermined.

Keywords: illuminated manuscripts; multi-analytical approach; non-invasive technique; iron-gall ink

Check for updates

Academic Editor: Georgios Karagiannis

Received: 9 May 2026
Revised: 22 June 2026
Accepted: 10 July 2026
Published: 16 July 2026

Copyright: © 2026 by the authors. Licensee MDPI, Basel, Switzerland. This article is an open access article distributed under the terms and conditions of the Creative Commons Attribution (CC BY) license.

1. Introduction

This study adopts an iterative workflow in which autoptic and structural examination guide targeted analytical investigations, whose outcomes are then interpreted alongside

textual, material, ornamental, and historical evidence. The specific research questions are outlined below.

1.1. Twelfth-Century Beneventan Manuscripts: Historical and Material Context

The twelfth century provides a particularly suitable setting for testing an integrated workflow on Beneventan manuscripts. In this period, manuscript production and use unfolded within a well-documented urban and institutional environment and under conditions likely to have shaped material choices, execution practices, and subsequent conservation trajectories. The political and social climate is framed by two major products of the city's written culture and a substantial collection of documents —the *Chronicon Beneventanum* (ChB) and the *Chronicon Sanctae Sophiae* (ChSS)—which provide a contextual baseline for interpreting the codices examined here [1–3]. Read together, these sources place local manuscript production within a city shaped by competing actors and recurrent tensions—heightened by episodes such as the schism of 1130—alongside processes of institutional consolidation and urban development that intensified across the twelfth century within a papal framework allowing a degree of local autonomy [4–6].

This historically and institutionally traceable setting is methodologically productive for three reasons. First, it includes phases of local production that remain comparatively underexplored, making them appropriate targets for renewed, evidence-led investigation. Second, the corpus preserved in the Benevento Cathedral Chapter library (BCB) forms coherent clusters of related codices whose shared paleographical, codicological and decorative features enable group-level comparison within relatively narrow chronological windows [7–13]. Third, the combination of a well-defined institutional setting and a strongly local liturgical tradition create favorable conditions for integrating experimental evidence from non-invasive diagnostics, to reconstruct materials, techniques, and later interventions in a controlled comparative framework. Where chronological attribution rests on ongoing paleographical assessment, it is treated as a working hypothesis to be tested against the integrated evidence.

1.2. From Visual Examination to Targeted Diagnostics

In situ non-invasive analyses can characterize only selected folios and features within a manuscript or related series; an analytical framework is therefore needed to organize findings at the appropriate scale. The analysis has been therefore organized around an operational unit, the Manuscript Production Environment (MPE), defined here as the set of materials and techniques used in the production of a manuscript or a coherent group of manuscripts identified through shared paleographical, codicological, and decorative features. A first characterization of the MPEs considered here can take the form of a basic inventory of the materials and techniques employed, considered as useful markers for future internal comparisons with other manuscript papers, and external ones with other case studies. Within this framework, the workflow proceeds iteratively: autoptic and structural examination guides the selection of targets for *in situ* non-invasive analyses; analytical outcomes are then reintegrated into revised manuscript descriptions, informed by existing cataloguing records and recent scholarship on Benevento's manuscript production. By producing more structured and comparable data, these descriptions may contribute to the enrichment of digital environments for manuscript study and cataloguing.

The new autoptic survey addresses four main domains in which relevant markers can be identified: (i) script features; (ii) codicological structure and material composition; (iii) pigments and ornamentation; and (iv) conservation state. Analysis is then defined through a threefold set of constraints: research priorities, logistics of *in situ* instrument set-up and conservation requirements. The protocol combines point-based elemental

spectroscopy with molecular spectroscopies, Vis-NIR hyperspectral imaging and high-magnification microscopy, applied to selected diagnostic targets on a limited number of folios. The resulting dataset supports the reconstruction of materials, execution techniques, and conservation issues for the analyzed units and—cautiously, by analogy—for closely related sections; broader generalization remains contingent on further campaigns and continued refinement of the workflow.

1.3. Research Questions

This workflow is designed to use integrated structural and diagnostic evidence to address the following questions in the selected case studies:

- RQ1: What are the materials used as pigments, binders and inks within the identified production contexts?
- RQ2: Is there evidence of underdrawings in the execution of the illuminated initials?
- RQ3: To what extent can external residues observed on the folios be associated with production activities, subsequent use/handling, or long-term storage?
- RQ4: Can materials inventory be established for each identified Manuscript Production Environment based on integrated evidence?

The case studies and research questions outlined contribute to a broader objective: reconstructing manuscript production environments through integrated structural, textual, material, and ornamental evidence. The data here shown will be hosted in the "Illuminated Manuscripts Hub", a digital platform offering access to heterogeneous data, tools and advanced digital services for the study, and enhancement of illuminated manuscripts [9,10].

2. Materials and Methods

2.1. Beneventan Manuscripts

The autoptic survey of the Beneventan manuscript collection preserved in the BCB, informed by existing cataloguing descriptions and recent scholarship, has made it possible to divide the collection into groups of manuscripts sharing various textual, codicological and historical-artistic affinities. Among these groups, two were selected for the first diagnostic investigations, resulting in a total of three manuscripts subjected to the full set of non-invasive techniques chosen for the study.

2.1.1. BCB 7 and 17 "Santorale"

The first group comprises Mss. 4, 7, and 17; BCB 1 may be added in the future should the proposed affinities be conclusively confirmed [8]. In any case, some gatherings belonging to BCB 4 were bound in BCB 1 during the reorganization desired by Vincenzo Maria Orsini at the beginning of the 18th century [11]. These manuscripts are hagiographic lectionaries belonging to a sanctorale arranged *per circulum anni* according to the Beneventan liturgy, realistically the only surviving witnesses of a much larger work that has otherwise been lost. Of the three, only Mss. 7 and 17 have so far been included in the diagnostic campaign (see Figures 1 and 2), whereas Ms. 4, already investigated from philological and art-historical perspectives [12], is scheduled for a forthcoming round of acquisitions.



Figure 1. Manuscript 7. (**a**) f. 25 r; (**b**) f. 67 r. Analytical points investigated by multi-analytical tecniques are indicated by the labels. Representative HRDM images are reported on the right side.



Figure 2. Manuscript 17 f. 30 r. Analytical points investigated by multi-analytical techniques are indicated by the labels. Representative HRDM images are reported on the right side, where in (Y2) the pink (#) and yellow (*) areas are labelled.

Content analysis shows that the chronological sequence of the readings is the reverse of the current shelf order. BCB 17 opens the series with the Pseudo-Ambrosius' *De Trinitate* (ff. 1 r–30 r) and the readings for saints' lives and passions from 30 November to 10 January. After a lacuna, the sanctorale continues in BCB 7 with readings from 17 January to 16 February. Structural evidence for the individual codices links their production to a single, coherent design project, carried out in the second half of the 12th century, according to the dating of the Benevento recension of the *Translatio sancti Nicolai*, identified between 1151 and 1190, whose text is contained in the sheets of BCB 4 bound in BCB 1, ff. 251 ra-256 vb [13,14]. The new observations appear to corroborate the hypotheses of unitary composition, particularly since pigment-use strategies in major initials and in distinctive initials. The decorative programs of the two lectionaries display a notable uniformity in both ornamentation types and stylistic choices; however, certain differences even within the individual codices warrant closer analysis. The manuscripts feature numerous illuminated initials on reserved parchment, positioned at the beginning of readings. These letters are red-profiled and coloured in various shades of green, blue, light blue, red, yellow, pink, and grey. In the brief notes provided by the studies on the decoration of these volumes, these were compared to 12th-century Beneventan script codices from Campania, decorated with initials of Beneventan-Cassinese culture, and updated with motifs of Apulian origin [15,16]. Most initials feature a dynamic interplay of elongated lanceolate leaves, multi-lobed palmettes, heart-shaped leaves, and scrollwork filling the interior spaces. Loosely woven interlaces mark the joints or, rarely, define some segments. The endings are often enlivened by zoomorphic protomes and, on rare occasions, by anthropomorphic heads (Ms 7, f. 67 r, Figure 1b). Human-headed terminals are considered a true "marchio di fabbrica" of Bari

illumination. These motifs also spread to the other side of the Adriatic from the mid-11th century [17]. Less common are the phyto-zoomorphic letters, formed by combining plant and animal elements, including the traditional dogs (Ms. 7, ff. 26 v, 86 r) and a large eagle forming the V of *Videte* on f. 86 r.

The diagnostic acquisitions were focused on ff. 25 r and 67 r (see Figure 1a,b), as determined by the research questions that emerged, the logistical constraints discussed above (Section 1.2), and considerations related to the decorative apparatus.

2.1.2. BCB 19 "Messale-Breviario"

The second group of manuscripts consists of BCB 19 and 20, a twelfth-century neumed breviary-missal in two parts (winter and summer). The temporale and sanctorale transmitted by these codices are kept separate. The sanctorale, characteristically Beneventan and most likely intended for the liturgy of the Cathedral Chapter, shows signs of influence from Montecassino's liturgical tradition (Masses for the feasts of St Maurus, St Scholastica, and St Benedict). The breviary follows the Roman cursus and employs a fully diastematic Beneventan system of notation, based on the placement of neumes at differentiated pitch levels. Due to the precarious conservation state of BCB 20, only Ms. 19 was subjected to the full set of non-invasive analyses (see Figure 3).

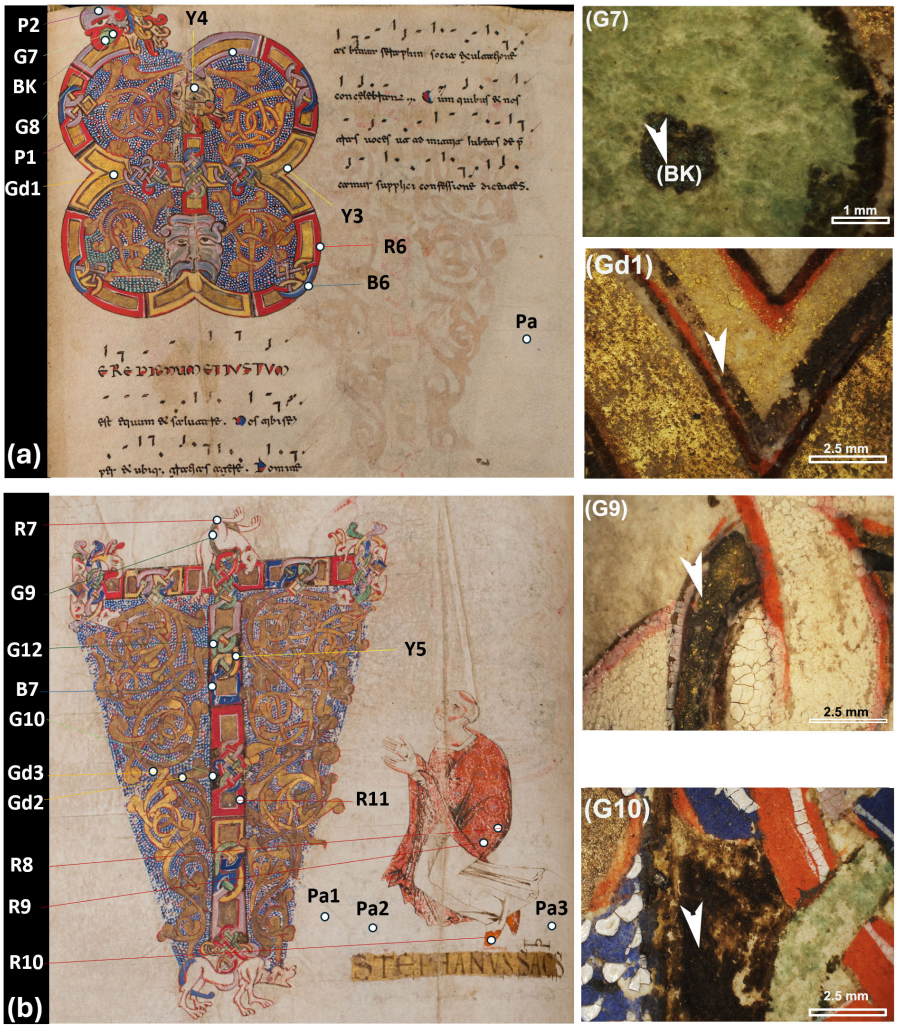

Figure 3. Ms. 19. (**a**) f. 108 r; (**b**) f. 108 v. Analytical points investigated by multi-analytical techniques are indicated by the labels. Representative HRDM images are reported on the right side *showing details of the preparatory sketches (G7 and Gd1) and green areas (G9 and Gd10) (white arrow).*

BCB 19 contains the winter portion of the breviary-missal, of which Ms. 20 constitutes the summer section. The two volumes are considered among "i più fedeli casi di adesione" of Beneventan illumination from the first half of the 12th century to the renewed decorative style developed at Montecassino during the Desiderian period (1058–1086) and codified in the Oderisian period (1087–1105). These are manuscripts that can be traced back to the same cultural context that gave rise to the famous *Chronicon Sanctae Sophiae* [18] and the breviary containing the *Calendarium beneventanum* of S. Sophia [19], to name a few manuscripts of certain Beneventan provenance, and perhaps the illuminated Exultet roll, Casanatense 724 (B I 13) 3 [20].

Two of the most sumptuous decorations of the manuscript 19 were subjected to an integrated multi-analytical investigation, containing respectively the monogram VD of *Vere Dignum* (f. 108 r, Figure 3a) and the large initial T of the *Te igitur* (f. 108 v, Figure 3b). Due to the poor condition of the second volume, it was not possible to carry out instrumental analyses, which would have enabled a comparative analysis useful for research purposes.

The monogram consists of gilded compartments connected by loose knots. The upper end of the left loop features a bird of prey's head. At the points of connection, masks and interlacing motifs face each other, framing the central cross. The interior contains gilded branches outlined in red ink, set against a blue and green base dotted with white.

Like the monogram, the initial T introducing the Canon of the Mass is divided into gilded compartments adorned with knots and set against a blue background dotted with white and enlivened by golden tendrils sprouting symmetrically from the dog's heads positioned at either end of the horizontal segment. Kneeling at the foot of the cross is a cleric, identified by the inscription on the golden band as *Stephanus sacerdos*, who may plausibly be the patron who donated the two volumes to the cathedral.

2.2. Analytical Techniques

In this study, a dedicated analytical setup was developed to ensure optimal instrument configuration and measurement reproducibility throughout the examination of the manuscripts. For High Resolution Digital Microscopy (HRDM), X-ray fluorescence (XRF), and Raman spectroscopy analyses, a horizontal stage equipped with an extendable arm was employed to provide stable and consistent instrument positioning (see Figure 4). Manuscripts were placed on a micrometric X–Y translation platform, enabling precise repositioning of the support between measurements without moving the manuscript itself, thus *minimising* the risk of mechanical stress or accidental displacement. Each folio was investigated at approximately 40 analytical points (including all techniques), selected to represent the range of pigments, the support, and the ink. An acquisition protocol was adopted, whereby non-invasive imaging techniques, specifically HRDM and hyperspectral imaging in the visible and *near infrared* (HSI Vis-NIR) range, were first employed to guide the selection of areas of interest for subsequent point analyses.

2.2.1. High Resolution Digital Microscopy (HRDM)

3D digital microscope (Hirox, Co., Ltd., Tokyo, Japan) (HRX-100 main unit) equipped with a 2.38 Mega-pixel CMOS sensor mounted on a stage combined with a motorized *Z*-axis enabling the investigation of the manuscripts directly in its horizontal display position (see Figure 4a). The images were acquired out at 30×, 50×, 140× and 350×, corresponding to FOVs of 11.4 mm, 5.5 mm, 2.09 mm and 0.82 mm and resolutions of 6.96 µm, 3.41 µm, 1.28 µm, and 0.50 µm respectively.

2.2.2. X-Ray Fluorescence

Elemental analysis of the illuminated manuscript was performed using F-70, a portable XRF spectrometer specifically designed and assembled at the CNR-ISPC by one of the

authors, for non-invasive investigations of cultural heritage materials (Figure 4b). The instrument is equipped with a tungsten (W) anode X-ray tube operating at 70 kV and 55 μA (MOXTEK, Inc., Orem, UT, USA). The high excitation voltage allows for the efficient excitation of medium- and high-Z elements typically present in historical pigments and metallic decorations (e.g., Pb, Cu, Fe, Hg, and Au). Spectra were acquired in 100 s, keeping the detector dead time below 20%. Fluorescent radiation was detected using a 20 mm^2 silicon drift detector (SDD, KETEK GmbH (Munich, Germany)), which provided adequate energy resolution for identifying characteristic emission lines. Spectra were processed using PyMCA software (version 5.9.2). A total of 70 measurements were performed. All XRF measurements were performed on the folios following careful inspection to exclude any contributions from ink writings or other decorative elements present on the verso side.

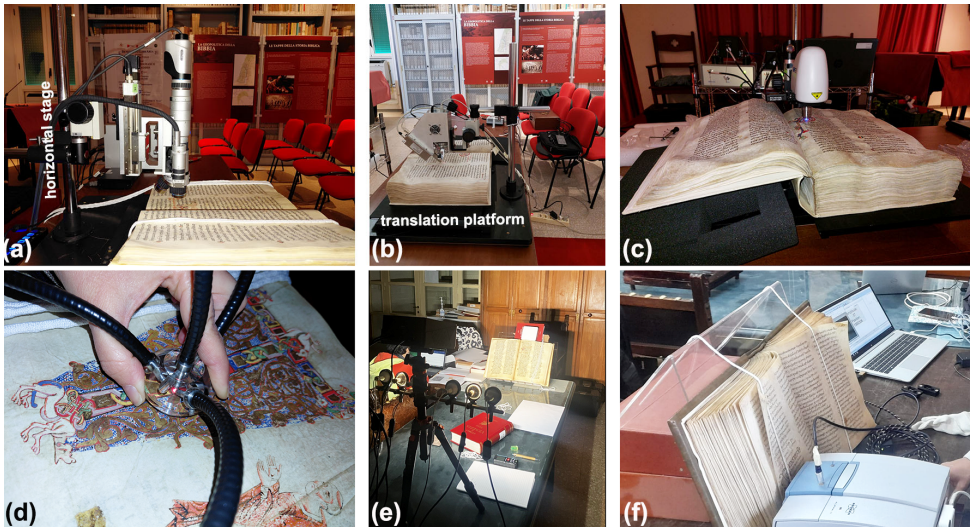

Figure 4. Analytical setup and multi-technique workflow adopted for analysis: (**a**) HRDM; (**b**) XRF; (**c**) Raman spectroscopy; (**d**) Vis–NIR reflectance spectroscopy; (**e**) HSI Vis-NIR; (**f**) FTIR.

2.2.3. Raman Spectroscopy

Raman measurements were performed using a portable spectrometer (B&W Tek, Newark, DE, USA) equipped with two different laser sources, at 785 nm (nominal output power 300 mW) and 532 nm (nominal output power 50 mW). The backscattered light is dispersed by an 830 line/mm and 1800 line/mm grating respectively, and the Raman signal is detected by a thermoelectrically cooled CCD array. The nominal spectral resolution is approximately 5 cm^{-1}, and the spectral range is 120–4000 cm^{-1}. Single-point acquisitions were performed with up to 50 accumulations, and an integration time of 1 s. All measurements were carried out in a micro-Raman configuration using 20× and 40× microscope objectives (spot diameters ~85 μm and ~50 μm, respectively). Laser powers were kept within ranges commonly reported for the analysis of light-sensitive heritage materials [21–23]. At 532 nm, powers ranged from 2.4–3.3 mW (20×) and 2.1–3.6 mW (40×); for the 785 nm laser, spectra were acquired at the minimum power setting available on the instrument (~4.8 mW and ~4.0 mW for the 20× and 40× objectives, respectively). The absence of visible photo-induced alterations was verified using the instrument's microscope camera, which allowed visual inspection of each area before and after acquisition and systematic recording of a post-acquisition image confirming the absence visible surface alterations.

During acquisitions, automatic dark subtraction is applied to remove interferences originating from the instrument, substrate interactions, or external light sources. OriginPro version 8.5 software was used for data processing, including baseline correction and smoothing.

2.2.4. Fourier Transform Infrared Spectroscopy (FT-IR)

In situ non-invasive infrared investigations have been carried out with a portable contactless Bruker Alpha spectrometer (Bruker, Milan, Italy) (Figure 4f) which is equipped with a reflection module with optical layout of 22°/22°, and a working distance of 1 cm ca. from the manuscript surface. Manuscripts were placed on a book stand, positioned so that the surface was perpendicular to the instrument's optical axis. Spectra were acquired from an area of 6 mm in diameter operating in the 7500–370 cm^{-1} range. 128 scans, with a resolution of 4 cm^{-1}, were performed for each measurement. Spectra are presented as log(1/R) (a.u., normalized in the range 0–1 for comparison) where R = reflectance, and for each spectrum a background measurement was acquired to subtract environmental contributions such as humidity and CO_2. Spectra were processed with Opus 8.5 software and OriginPro version 10.3.

2.2.5. Vis-NIR Reflectance Spectroscopy

Reflectance spectroscopy measurements in the visible and near-infrared (Vis–NIR) spectral range were carried out using a portable Zeiss spectrometer integrating two modules: the MCS 601 UV-Vis and the MCS 611 NIR 2.2 WR, mounted on a common optical bench (Figure 4e). The instrument operates over the spectral range 200–2200 nm; under the standard acquisition configuration adopted for this study, reflectance spectra were recorded across the range 350–2200 nm. The spectral sampling interval was 0.8 nm/pixel in the 350–980 nm region and approximately 5 nm/pixel in the 980–2200 nm region. Measurements were performed using a hemispherical probe with a 0°/45°/45°/45° illumination and collection geometry, yielding a circular sampling area of approximately 2 mm in diameter. Calibration was performed using a 99% reflective Spectralon® white reference target (Labsphere Inc., North Sutton, NH, USA), and spectral data were processed using Zeiss Aspect Plus® version 2.10.3. software.

2.2.6. Hyperspectral Vis–NIR Imaging

Reflectance imaging spectroscopy was performed using a portable Vis–NIR hyperspectral imaging system (HERA, NIREOS S.r.l., Milan, Italy) operating in the 400–1000 nm spectral range (Figure 4e). The system is based on a Fourier-transform (FT) approach and incorporates a patented common-path birefringent interferometer (CPI) coupled to a monochrome silicon CMOS detector (1280 × 1024 pixels). The system provides a spectral sampling of approximately 5 nm, with an effective spectral resolution of <1.5 nm at 400 nm and <10 nm at 1000 nm, resulting in 120 spectral channels across the investigated range. The optical configuration includes a 25 mm focal length objective (maximum aperture f/1.85), providing a field of view of 8° and a working distance ranging from 60 cm to infinity.

The compact device was mounted on a tripod along with an illumination system, which provided a low-voltage (12 V) hybrid array consisting of four 7 W white LEDs (6000 K, 450 lm each, LACMISC, Shenzhen, Guangdong, China) and two 35 W warm halogen lamps (2900 K, 314 lm each, Halogen Reflektor Security, Paulmann Licht GmbH, Springe, Germany). This hybrid configuration yielded continuous spectral coverage across the visible and near-infrared regions (400–1000 nm).

Hyperspectral data-cubes were acquired by recording interferograms at different interferometer positions and reconstructing pixel-wise spectra via Fourier transformation, yielding a three-dimensional dataset (x, y, λ).

Acquisition parameters, detail reported in Supplementary Materials (Table S1), including exposure time, number of averages, and working distance, were adjusted for each folio to optimize signal quality and ensure appropriate spatial coverage.

Radiometric calibration was performed using a Spectralon diffuse reflectance standard (5-inch, 99% reflectance, Labsphere, Inc., North Sutton, NH, USA) to normalize the hyperspectral data. In addition, flat-field correction was carried out using a white cardboard sheet (A3 format, 250 g m^{-2}) placed under identical illumination conditions to compensate for spatial non-uniformities in illumination and detector response. The resulting data-cubes were exported in ENVI format (version Classic 5.1) for subsequent processingTo enhance data quality and reduce noise, the calibrated spectral cubes were subjected to a Minimum Noise Fraction (MNF) transformation, a standard pre-processing step in hyperspectral imaging that separates noise from meaningful spectral information and retains the most significant bands for subsequent analysis [24]. The MNF-transformed cube was then processed using Sequential Maximum Angle Convex Cone (SMACC) algorithm [25], an automated routine to extract spectrally distinct features (endmembers) to subsequently classify pixels via the Spectral Angle Mapper (SAM) algorithm [26]. Additionally, first-derivative spectral cubes were computed to enhance transition edges and absorption features and improve discrimination between spectrally similar pigments [27].

3. Results

A non-invasive, multi-analytical approach was applied to characterise the material (pigments, binders, inks) across the three examined manuscripts. A comprehensive summary of constituent materials identified across all three manuscripts is provided in Table 1.

3.1. Manuscripts BCB 7, 17: "Santorale"

3.1.1. Ink

A black ink was used throughout the written text of both manuscripts, whereas a brown ink was employed for preparatory sketches and selected decorative details (Figure 5). HRDM observations revealed differences in the execution of these drawings, which appear darker and more defined in Ms. 17 and almost transparent in Ms. 7 (white arrow in Figure 5). Hyperspectral imaging in the Vis–NIR range identified, in both manuscripts, a spectral endmember associated with the written text (Figure 6), displaying a reflectance profile typical of iron-gall ink, characterized by strong absorption throughout the visible region and a marked increase in reflectance in the near-infrared range [28]. This attribution was supported by XRF analyses showing Fe and K, with minor Cu, and by Raman spectra displaying the characteristic iron-gall inks bands at 1336, 1487, and 1584 cm^{-1}, together with a broad feature at 550 cm^{-1} (Table 1 and Supplementary Material Figure S1). The band observed at 1487 cm^{-1} is slightly shifted with respect to the value reported in the literature (~1475 cm^{-1}) [29], a variation that has been hypothesized to be associated with differences in ink formulation, pH, iron-to-ligand ratio, or tannin source [30–33]. This spectral displacement reflects the chemical complexity inherent to iron-gall inks, whose composition varied considerably depending on the raw materials and recipes available to medieval scribes.

Table 1. Summary of the results obtained by the multi-analytical analysis: Raman spectroscopy, XRF, Vis–NIR reflectance spectroscopy, and FTIR spectroscopy. ND = not detected; NA = not available.

Colour	Analytical Point	Manuscript	Identified Material	Raman Bands (cm^{-1})	XRF	Vis–NIR Reflectance (nm)	FTIR Bands-Binder (cm^{-1})	FTIR Bands-Pigment (cm^{-1})	Proposed Binder
Red	*R1, R2, R3, R4, R5, R6, R7, R8*	Ms. 7, Ms. 17, Ms. 19	Cinnabar (HgS)	254, 285, 343	Ca, Fe, Hg, Pb	R_edge at 598	1020 (saccharide-based) 1567 (1545 shoulder), 1683 (protein), 2853, 2927, 2955, 4253, 4330 (lipid)	ND	Proteinaceous/lipidic/saccharide -based in some areas
Red-orange	*R9, R10*	Ms. 19	Minium (Pb_3O_4)/Cinnabar (HgS)	121, 150, 391, 550	Ca, Hg, Pb	R_edge at 561	2853, 2927, 2955, 4250, 4330 (lipid)	ND	Lipidic and/or proteinaceous
Pink	*Pi*	Ms. 17	Probable organic lake + cinnabar	NA	Ca, Fe, Hg, Pb	R_edge at 598	NA	NA	NA
Purple	*P1, P2*	Ms. 19	Red lake + lead white	Lead white band at ~1049	Ca, Fe, Hg, Pb	R_edge at 626	NA	NA	NA
Dark blue	*B2, B3, B5, B6*	Ms. 7, Ms. 17, Ms. 19	Natural ultramarine	545, 1316	Ca, Fe, Hg, Pb	Abs at 600	1020 (saccharide-based)	2340 (natural ultramarine), 680, 830 (lead white)	Proteinaceous
Light blue	*B1, B4,*	Ms. 7	Ultramarine + lead white	545, 1049, 1316	Ca, Fe, Hg, Pb	Abs at 600	1470, 1730 (lipid), 1685 (protein)	2340 (natural Ultramarine)	Lipidic and/or proteinaceous
Green	*G1, G2, G3, G4, G5, G6, G7, G8*	Ms. 7, Ms. 17, Ms. 19	Copper-based green pigment	Fluorescence	Ca, Fe, Cu, Hg, Pb	R_max at 556 R_sh at 667 Abs at 715 nm in Ms. 7, R_max at 532 nm Abs at 745 nm in Ms. 17	1020 (saccharide-based) 1567 (1545 shoulder), 1683 (protein), 2853, 2927, 2955, 4253, 4330 (lipid)	ND	Proteinaceous/saccharide-based
	G9	Ms. 19	Probable ink mixed with Orpiment (As_2S_3)	158, 206, 295, 313, 357, 386	Hg, As/Pb	Broad R_max at 551	1020 (saccharide-based), 1545, 1685 (protein)	597, 670, 1120 (sulphates)	Proteinaceous/saccharide-based
	G10		Iron-gall ink	550, 1336, 1488, 1579	Ca, Fe, Cu, Hg, Pb	ND	1020 (saccharide-based), 1545, 1685 (protein)	ND	ND
Yellow	*Y1*	Ms. 7	Brown ink	NA	K, Ca, Fe, Cu, Hg, Pb	Increase refl. from 500	NA	NA	NA
	Y2	Ms. 17	Probable yellow organic lake	939, 1421 1003 (probably phenylalanine)	K, Ca, Fe, Cu, Hg, Pb	R_sh at 586	1020 (saccharide-based)	NA	Proteinaceous/saccharide-based
	Y3, Y4, Y5	Ms. 19	Orpiment (As_2S_3)	158, 206, 295, 313, 357, 386	Ca, Fe, Au, Hg, As/Pb	R_edge < 500	ND	1118 (sulphates)	ND
White	*W1, W2,*	Ms. 7	Lead white	1049	Ca, Fe, Hg, Pb	ND	1470, 1730 (lipid), 1685 (protein)	680, 830 (lead white)	Lipidic and/or proteinaceous
Text	*L1, L2, L3, L4, L5, L6*	Ms. 7, Ms.17	Iron-gall ink	550, 1336, 1487, 1584	K, Ca, Fe, Cu Zn	Strong abs. in Vis, increased refl. after 700	1020 (saccharide-based)	ND	Saccharide-based
Sketches	*Hyperspectral map*	Ms. 7, Ms. 17, Ms19	Probable diluted iron-gall ink	NA	NA	increase refl. from 500	1020 (saccharide-based)	ND	Saccharide-based
Gold decoration	*Gd1, Gd2, Gd3*	Ms. 19	Gold with minor Ag	NA	Ca, Fe, Cu, Au, Hg, Pb, Ag	NA	NA	NA	NA

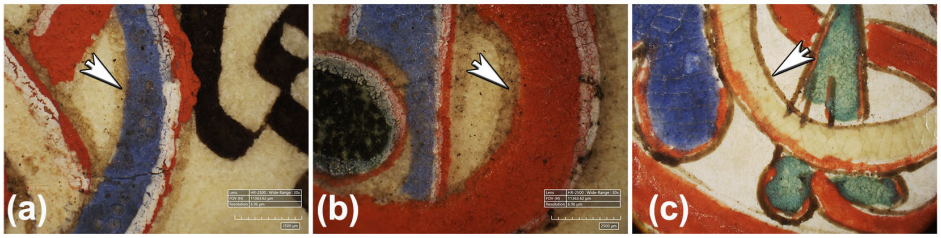

Figure 5. High-resolution digital microscopy (HRDM) images showing details of the underdrawings (white arrow) in: (**a**) Ms. 7, f. 25 r; (**b**) Ms. 7, f. 67 r; (**c**) Ms. 17, f. 30 r.

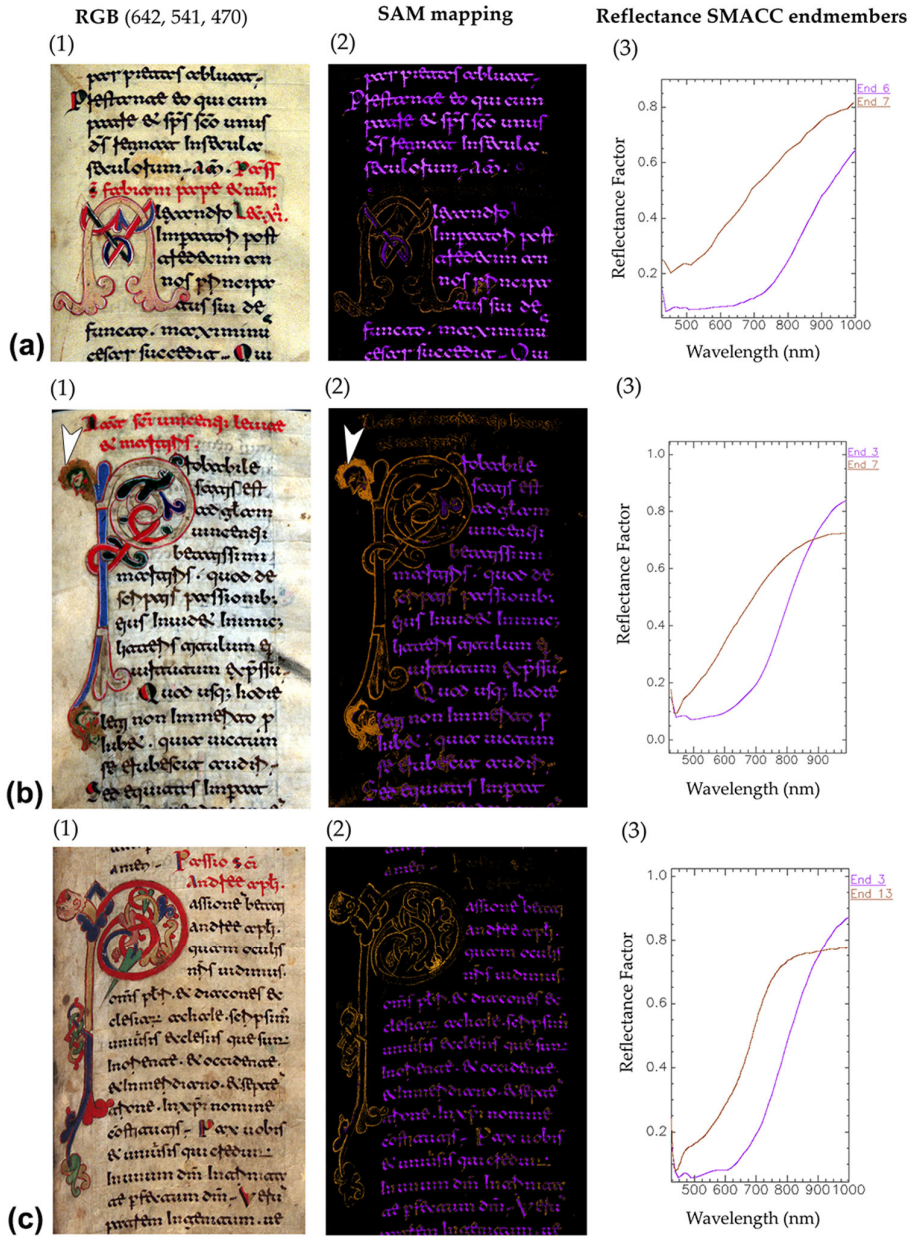

Figure 6. RGB image of the Folio 25 r (**a1**), 67 r (**b1**) of Ms. 7 and 30 r (**c1**) of Ms. 17 reconstructed from the 642 nm, 541 nm, and 470 nm bands of the hyperspectral datacube; SAM classification maps for folios 25 r (**a2**), 67 r (**b2**) and 30 r (**c2**) using ink-related endmembers extracted by SMACC routine (**a3**,**b3**,**c3**). White arrow indicates the yellow anthropomorphic protomes figures.

FTIR further indicated the presence of a saccharide-based binder (Table 1, Supplementary Material Figure S1) [34,35].

Hyperspectral imaging of Ms. 7 (ff. 67 r and 25 r) additionally revealed the occurrence of the iron-gall spectral endmember within the blue and green regions of the illuminated initials A and P (Figure 6). The spatial correspondence between these coloured areas and the iron-gall signature suggests that the ink was used either as an underdrawing material or mixed with pigments to modify their tonality, a practice documented in medieval manuscript illumination [28].

A second spectral endmember was associated with preparatory sketches and the yellow-brown details of the anthropomorphic protomes (white arrow in Figure 6b). Unlike the iron-gall endmember, it exhibited a gradual increase in reflectance beginning at approximately 500–600 nm. A similar spectral behaviour was also observed in faded portions of the written text, suggesting that ink alteration phenomena may contribute to this response. Although this brown ink can be clearly distinguished from iron-gall ink on the basis of its spectral signature, the available analytical data do not allow its composition to be conclusively identified. Finally, parchment support was *characterised* by FTIR and XRF; full spectral data and interpretation are reported in Supplementary Materials (Section S1 and Figure S2) [36–38].

3.1.2. The Characteristic Palette Colors

Pigments and their binder were identified using XRF, Raman, Vis-NIR reflectance, and FT-IR analyses, performed in areas defined by the endmember maps obtained from hyperspectral analysis (Figure 7).

Reddish Hue

Red pigment was identified in the borders, decorative elements of the illuminated initials, and rubrics of all investigated folios (Figures 1 and 2 and Table 1). The red endmember (End2 in Figure 7) exhibits a characteristic S-shaped reflectance spectrum in the Vis–NIR range, with a sharp transition edge around 600 nm, which is typical of cinnabar (vermilion) (HgS), clearly resolved in the first-derivative spectra which show a distinct peak at approximately 598 nm [39] (Table 1 and Supplementary Material Figure S3). The identification was confirmed by XRF, which detected Hg as the main elemental constituent, and by Raman spectroscopy through the diagnostic bands at 254, 285, and 343 cm^{-1} (Table 1 and Figure S3) [40]. FTIR analyses of the red areas revealed the presence of lead white ($2PbCO_3 \cdot Pb(OH)_2$) and an organic binder. In detail, in folio 67, spectral features suggest a glycosidic component, consistent with a saccharide binder [35], alongside a proteinaceous component, which could also be related to the contribution of the support [35]. It is noted that the relative intensities of these combination bands are slightly higher in the pigmented rather than in the support spectrum (Supplementary Material Figure S3) [36]. Calcium oxalates were also identified and are interpreted as degradation products of the organic fraction [41]. As no lipid-related absorptions were observed [42], the binder was likely polysaccharide and/or protein-based [35,43] (Table 1). In contrast, the red areas of folio 25 exhibited a different FTIR profile, with additional bands suggesting possible variations in binder composition and the potential presence of a lipidic component (Table 1 and Supplementary Material Figure S3).

Blue Hue

Blue pigments were identified in the historiated initials and minor initials of both manuscripts (Figures 1 and 2 and Table 1). While Ms. 17 exhibits only a dark blue hue, two distinct blue tonalities, light and dark, are present in Ms. 7 (ff. 25 r and 67 r). Hyperspectral analysis identified a blue endmember (see Figure 7, End4 in a3 and c3, and End5 in b3) *characterised* by a broad absorption centred around 600 nm and a progressive increase in reflectance toward the near-infrared region, a spectral profile consistent with ultramarine

blue [39]. This identification was also confirmed by FTIR and Raman spectroscopy through the characteristic bands of natural ultramarine at 545 and 1316 cm^{-1} [44–46] (Table 1 and Supplementary Material Figure S4). In the lighter blue areas, Raman and FTIR analyses indicated the presence of lead white admixed with ultramarine (Table 1), consistent with the lighter appearance observed by HRDM (Figure 1 (B1–B3)). Regarding the binder, in Ms. 17 (f. 30.r) intense carbonate and parchment signals dominate spectral contribution, yet a shoulder in the amide II band could be attributable to a protein binder [43], and additional features to a lipid one (See Table 1), in spite of the absence of other related bands. A similar situation is observed in the blue areas of folio 25 and 67 of Ms. 7 [35].

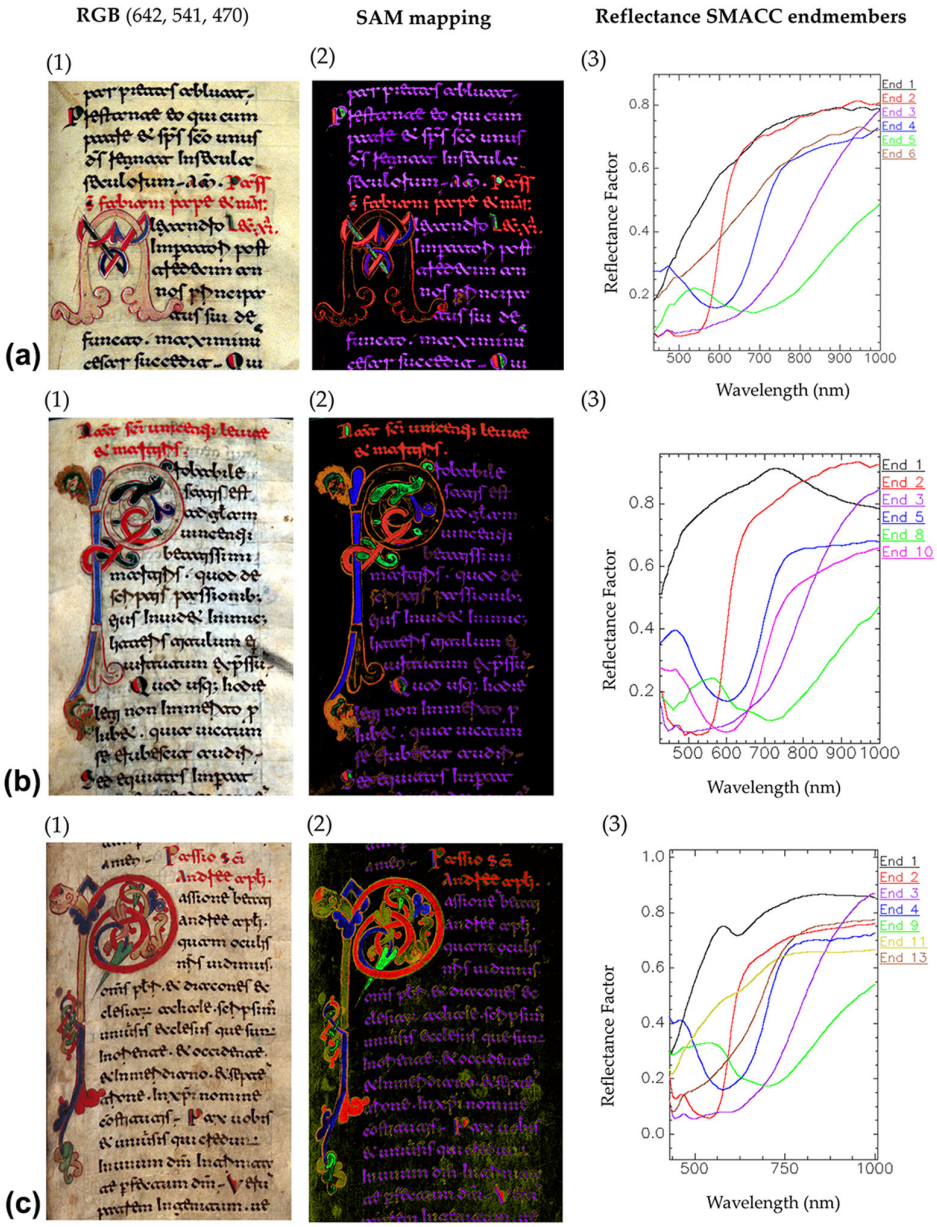

Figure 7. RGB image of the Folio 25 r (**a1**), 67 r (**b1**) of Ms. 7 and 30 r (**c1**) of Ms. 17 reconstructed from the 642 nm, 541 nm, and 470 nm bands of the hyperspectral datacube; SAM classification maps (**a2**,**b2**,**c2**) obtained using endmembers extracted from SMACC routine for the three folios (**a3**,**b3**,**c3**).

Green Hue

Green pigments were identified in the illuminated initials and minor initials of both manuscripts (Figures 1 and 2 and Table 1). In Ms. 7 (ff. 67 r and 25 r), the extracted

green endmembers (End5 and End8 in Figure 7) exhibit highly similar spectral behaviour, *characterised* by a reflectance maximum at approximately 556 nm, a secondary shoulder around 667 nm and a more characteristic absorption at 715 nm. This consistent spectral shape across both folios indicates a relatively homogeneous material response and suggests the use of a copper-based green pigment [39]. In Ms. 17 (f. 30 r), the green endmember (End9 in Figure 7) displays a different spectral response, *characterised* by a broader feature centred at approximately 532 nm and an absorption at 745 nm. Compared to Ms. 7, this spectrum appears less structured and more smoothed, suggesting differences in the optical response, which may reflect variations in pigment composition, concentration, or alteration state within a copper-based pigment system [47]. XRF analyses consistently detected high Cu counts in all investigated green areas, confirming the use of copper-containing materials (Supplementary Material Figure S5). HRDM observations revealed marked differences between the two manuscripts (Figures 1 and 2, (G1, G3, G5, G6)). In Ms. 7, the green paint appears semi-translucent and non-crystalline, with local brownish tonalities suggestive of alteration processes. In contrast, the green areas of Ms. 17 display a matt and discontinuous appearance, with partial exposure of the underlying layers. FTIR analyses excluded malachite owing to the absence of diagnostic carbonate features [48]. On the other hand, the exact identification of verdigris proved particularly challenging, as has been reported in previous studies [49], not primarily owing to overlapping matrix signals or spectral distortions, but likely because neutral and/or basic copper acetates dissolved over time within the binder, rendering them spectroscopically elusive. Raman analysis of the green areas yielded spectra dominated by a high fluorescence, which obscured most diagnostic features. Oxalate signals observed by FTIR, likely attributable to copper and/or calcium oxalates [41], are more intense than in the corresponding areas of Ms. 7 (both on f. 25 and f. 67 r).

Yellow Hues

Yellow pigment was identified in the inner decoration of the illuminated initials (see Figures 1 and 2 and Table 1). In Ms. 17, Hyperspectral mapping revealed a yellow endmember associated with the letter P (Figure 7), characterized by a spectral profile more consistent with an organic *colorant* than with a mineral yellow pigment. A notable characteristic is the gradual reflectance increase, the so-called "knee", occurring between 500 and 550 nm, a feature more consistent with an organic yellow lake than with a mineral one [39]. Raman spectroscopy did not provide evidence for inorganic yellow pigments but revealed bands that might possibly be attributed to proteinaceous materials [50] (Table 1), suggesting the presence of a protein-rich binding medium (Supplementary Material Figure S6). This interpretation may be further supported by HRDM observations (Figure 2, "Y2"), which reveal a coherent paint layer affected by fine craquelure, a visual feature consistent with literature describing the use of substantial quantities of proteinaceous binders in organic *colorant*, where they contribute to the cohesion and adhesion of the pictorial layer [51]. In contrast, no distinct yellow endmember was identified in the yellow-orange details of the anthropomorphic protomes in Ms. 7 (f. 67 r) (as pointed out by the white arrow in Figure 7b). Their spectral signature closely matches that of the brown preparatory ink, suggesting that these details were executed using the same material. XRF, Raman, and FTIR analyses did not provide conclusive evidence for an additional yellow pigment (Table 1). Therefore, the yellowish-orange appearance is tentatively attributed to the brown ink, either alone or in combination with unidentified compounds.

Pink Hues

A pink hue was observed in the inner decoration of the illuminated initial "P" in Ms. 17 (f. 30 r), displaying a glossy appearance similar to that of the yellow areas (labelled "#" in Figure 2 "Y2"). The reflectance spectrum exhibits the characteristic cinnabar absorption edge at approximately 596 nm. However, these areas are also mapped by the endmember associated with the yellow hue (Figure 7), suggesting that the pink tonality may result from the admixture of the organic yellow *colorant* with small amounts of cinnabar used for the outlines. XRF analysis detected Hg, Pb, and Fe (Supplementary Material Figure S7).

White Hues

White pigment was identified exclusively in Ms. 7, where it occurs in both investigated folios within the illuminated initials. XRF analyses revealed a strong Pb signal (Supplementary Material Figure S7) [52], while Raman spectroscopy identified the characteristic band of lead white at 1049 cm^{-1}; the assignment was further confirmed by FTIR spectroscopy (Table 1).

3.1.3. Conservation State: "External Residues"

Dark stains are visible across the Ms17, with variable size and thickness (see Figure 2 "S1"). The spectral signals indicate the presence of aliphatic long chains and esters of fatty acids, compatible with the presence of beeswax dripped onto the folio (See Figure 8) [53].

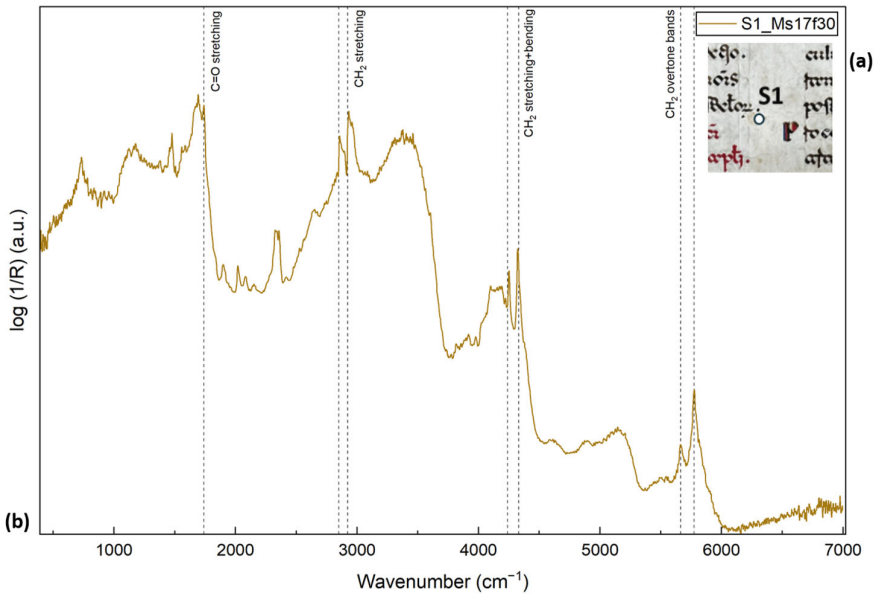

Figure 8. Detail of the stain "point S1" (**a**) and corresponding FTIR spectrum (**b**).

3.2. BCB 19: "Messale-Breviario"

3.2.1. Ink

A black ink was identified in the body text of 108 folio v/r, while a brown ink was employed for the underdrawings of the illuminated initial letters (Figure 7). HRDM shows that the preparatory sketches exhibit a darker appearance with a stroke definition (white arrow, Figure 3 "G7 "and "Gd1"). In addition, hyperspectral mapping showed that black ink was used not only as a writing medium but also as a pigment. This interpretation was corroborated by XRF and Raman (Figure 3 and Supplementary Material Figure S5). Its full compositional characterization is discussed in the dedicated section on individual pigments (see Section 3.2.2). Moreover, on folio 108 v, iron-gall ink was also used to define the delicate folds of the vestment of Stephanus Sacerdos (see Figure 9c), and appears to

have been mixed with other pigments to achieve green-brown tonalities. Finally, parchment supports were *characterised* by FTIR; full spectral data and interpretation are reported in Supplementary Materials (Section S1 and Figure S2).

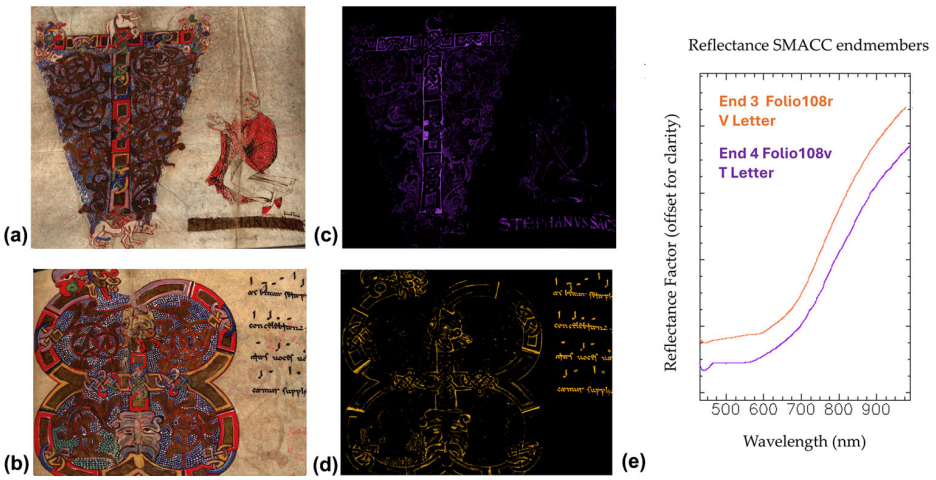

Figure 9. RGB images of the folio 108 verso (**a**) and recto (**b**) of Ms. 19 reconstructed from the 642 nm, 541 nm, and 470 nm bands of the hyperspectral datacube; SAM classification map obtained for verso (**c**) and recto (**d**) of folio 108; (**e**) endmembers extracted by SMACC routine performed on the reflectance cube.

3.2.2. The Characteristic Palette Colors

Reddish Hue

Red pigments were identified in the illuminated initials, the decoration of Stephanus' garment, and selected rubric areas (Figure 10 and Table 1). Multi-modal analysis identified cinnabar (HgS) as the primary red pigment, while FTIR spectra indicate a predominantly proteinaceous binding medium (Table 1 and Supplementary Material Figure S3).

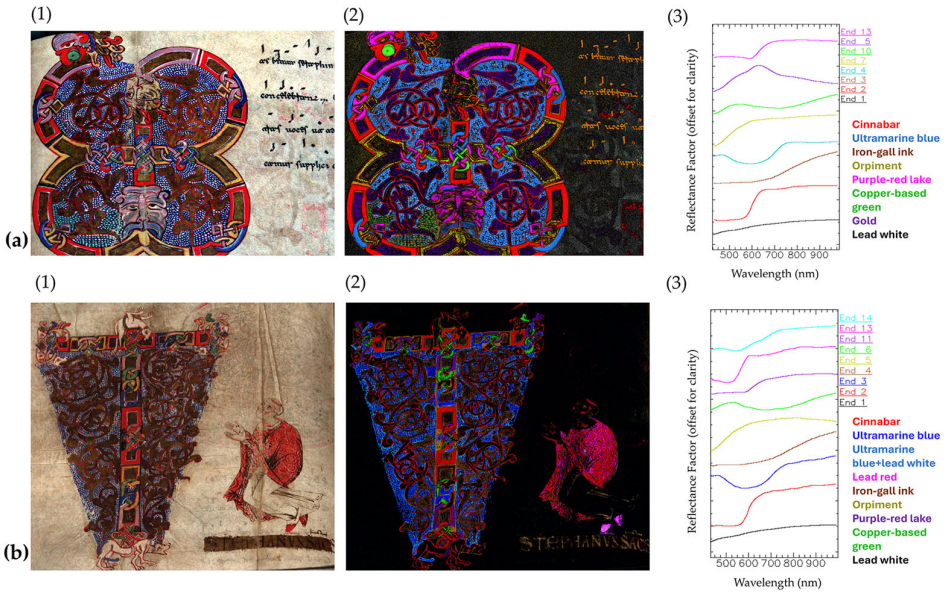

Figure 10. RGB image of the folio 108 recto (**a1**) and verso (**b1**) reconstructed from the 642 nm, 541 nm, and 470 nm bands of the hyperspectral datacube; SAM classification map obtained for recto (**a2**) and verso (**b2**) of folio 108; in (**a2**), lead white is showed in white, in (**b2**), orpiment and lead white are not shown for clarity of visualization. (**a3**,**b3**) endmembers extracted by SMACC routine performed on the reflectance cube.

Contrary, a more complex palette was observed in Stephanus' garment, where the main red areas consist of cinnabar, whereas the red-orange decorative element contains a mixture of cinnabar and red lead (Pb_3O_4). In contrast, the footwear was painted exclusively with red lead (Table 1 and Supplementary Material Figure S3). The spatial distribution of both pigments was visualized by hyperspectral imaging by mapping SMACC-derived derivative endmembers (Figure 11). FT-IR spectra acquired from the two red hues of the garment and shoes (points R9 and R10 in Supplementary Material Figure S3) reveal a variable lipid contribution (Table 1) [54].

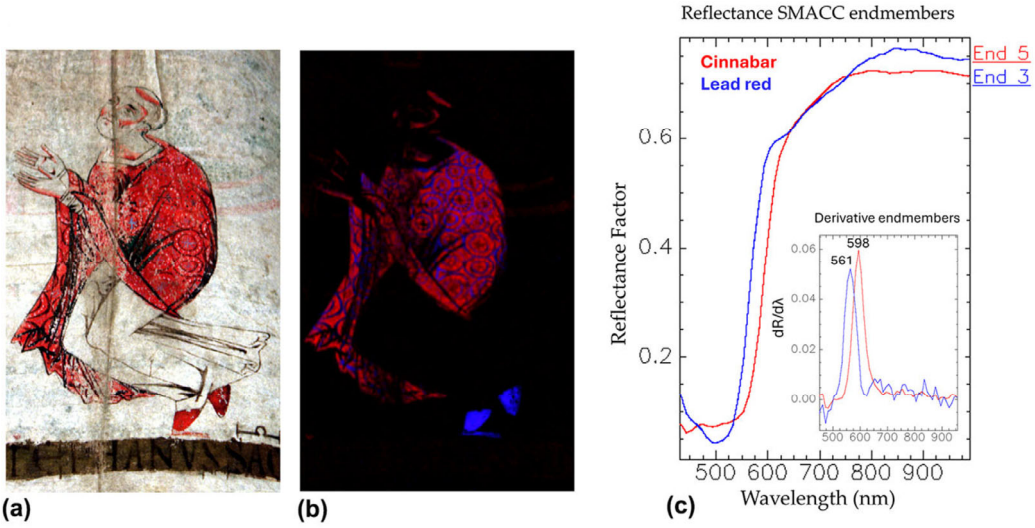

Figure 11. (**a**) RGB image of the detail of *Stefanus Sacerdos* in folio 108 v reconstructed from the 642 nm, 541 nm, and 460 nm bands of the hyperspectral datacube; (**b**) SAM classification map showing cinnabar (red) and red lead (blue); (**c**) endmembers extracted by SMACC routine, corresponding to red lead (endmember 3) and cinnabar (endmember 5).

Blue Hue

As in manuscripts examined above, the blue pigment was identified as natural ultramarine derived from lapis lazuli (see Table 1 and Supplementary Material Figure S4). Reflectance imaging spectroscopy (Figure 10) indicates that ultramarine was applied predominantly in pure form, with lead white used only locally in the illuminated "VD" (f. 108 r) to create lighter tonalities. In contrast, the blue decoration of the letter "T" on the verso is composed almost entirely of pure ultramarine (Table 1 and Supplementary Material Figure S4). Hyperspectral mapping additionally revealed ultramarine in the stars decorating the drapery of *Stefanus sacerdos*, a feature not evident by visual inspection alone (Table 1 and Figure 10).

Greenish Hue

Green pigments were employed across a range of hues in the illuminated initials "VD" and "T" (Table 1). Hyperspectral imaging and XRF analyses consistently indicate the use of copper-based green pigments throughout the decorations (Supplementary Material Figure S5); however, the available data did not allow unequivocal identification of the specific copper compound. Notably, a distinctive green hue was observed in the depiction of the dog (G9) and in the central area of the decoration on folio 108 v (G10) (White arrow in Figure 3). HRDM imaging of point G9 revealed yellow grains dispersed within a grey-green matrix (Figure 12), where Raman spectroscopy identified the orpiment (As_2S_3) occurrence [40] (Table 1 Supplementary Material Figure S5). FTIR spectra acquired in this area revealed bands consistent with sulphate groups (Figure 12a) [34], which may be attributed to *in situ* oxidation of sulfidic ions from orpiment or via local solubilization of other constituent

materials (e.g., gypsum) [55]. In contrast, XRF analysis did not detect any copper signal in the investigated area, indicating that the green-yellow tonality was not produced by a copper-based green pigment (Table 1 and Supplementary Material Figure S5). To further investigate the composition of this mixture, the dog figure was isolated and endmembers were extracted from the selected region using the SMACC algorithm (Supplementary Material Figure S8). Although the limited spatial extent of the feature constrains its contribution to the overall spectral signal, the dark endmember (endmember 3; Figure S8b) does not appear consistent with iron-gall ink, suggesting the possible presence of a black colourant distinct from iron-gall ink. Conversely, the dark green-brown area G10 (Figure 3) showed elevated Fe and Cu counts by XRF analysis. The high level of iron suggests that iron was an intentional constituent of the pigment composition (Supplementary Material Figure S5). In fact, Raman spectroscopy confirmed the presence of iron-gall ink in addition to gypsum occurrence in this area (Table 1 and Figure 12b).

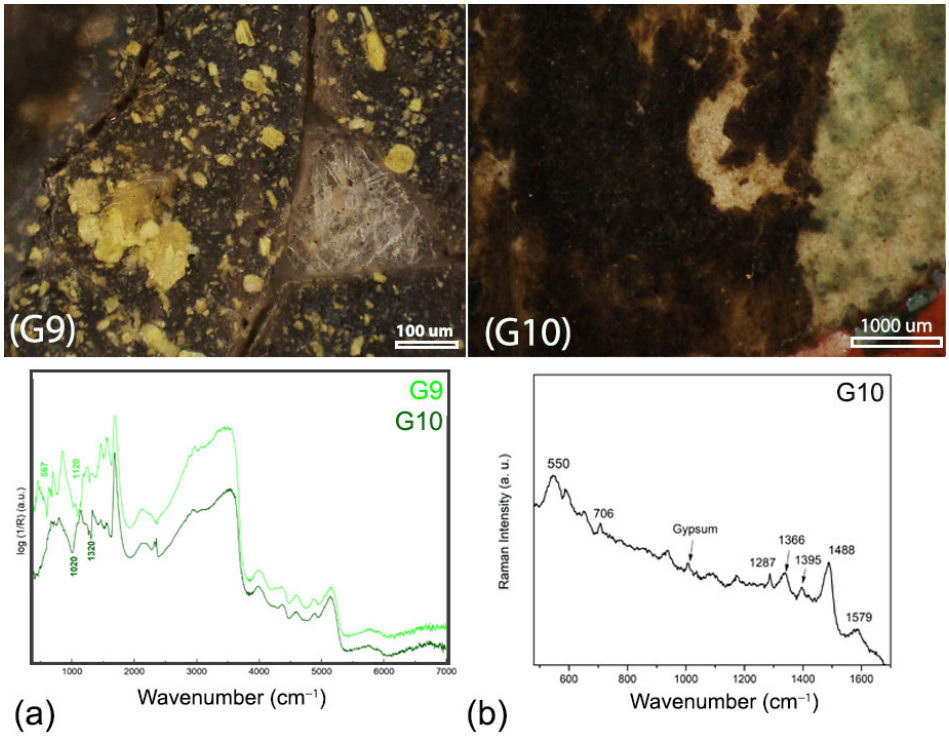

Figure 12. (**G9**) HRDM image revealing yellow grains of orpiment embedded within a dark grey-green matrix; (**G10**) HRDM image showing the dark green-brown area of the decoration; (**a**) FTIR spectra acquired at points G9 and G10; (**b**) Raman spectrum acquired at point G10.

Yellowish Hue

Hyperspectral imaging identified the presence of orpiment (As_2S_3) across the yellow areas on both folios (see Figure 10) based on its characteristic spectral features [39] in the Vis–NIR range, including a strong absorption edge in the blue region (below ~500 nm) and high reflectance in the yellow–red region, often accompanied by a broad reflectance plateau towards the NIR (Table 1). This assignment was confirmed by Raman spectroscopy (Supplementary Material Figure S6), while FTIR analysis revealed sulphate-related features consistent with the possible presence of sulphates, possibly related to orpiment sulphur ions oxidation (see "Greenish hues" Section 3.2.2) and/or gypsum [55] (Table 1 and Supplementary Material Figure S6).

Purple Hues

Purple hues were employed in the decoration of the illuminated initials on both sides of the folios (Figure 3 and Table 1). XRF analysis detected Hg and Pb in the purple areas; however, Raman spectroscopy did not identify cinnabar but only lead white (Table 1 and Supplementary Material Figure S7). HRDM imaging showed that cinnabar is restricted to the outlines of the decorations and adjacent red details, indicating that the Hg signal likely originates from neighbouring paint layers rather than from the purple pigment itself (Figure 13(2a)). Lead white was also identified, while the Cu detected at point 1a (Figure 13) is attributable to a copper-based green pigment superimposed on the purple layer. Hyperspectral imaging further demonstrates that the purple decorations do not result from a mixture of cinnabar and ultramarine blue although it is present in details such as the forehead and mouth of the "monstrous head" (Figure 13b). First-derivative spectra display features characteristic of a red lake, including a broad absorption band *between 550–600* nm and increased reflectance in both the blue and red regions (Figure 13d). This *behavior*, together with a transition edge at approximately 626 nm, supports the presence of an organic chromophore. Comparison with reference datasets reveals similarities with red–purple lake pigments, particularly when considering the apparent absorbance spectra with maxima at 556 and 581 nm [39,56,57] (see Supplementary Materials Figure S9); however, a specific attribution remains challenging based on reflectance data alone.

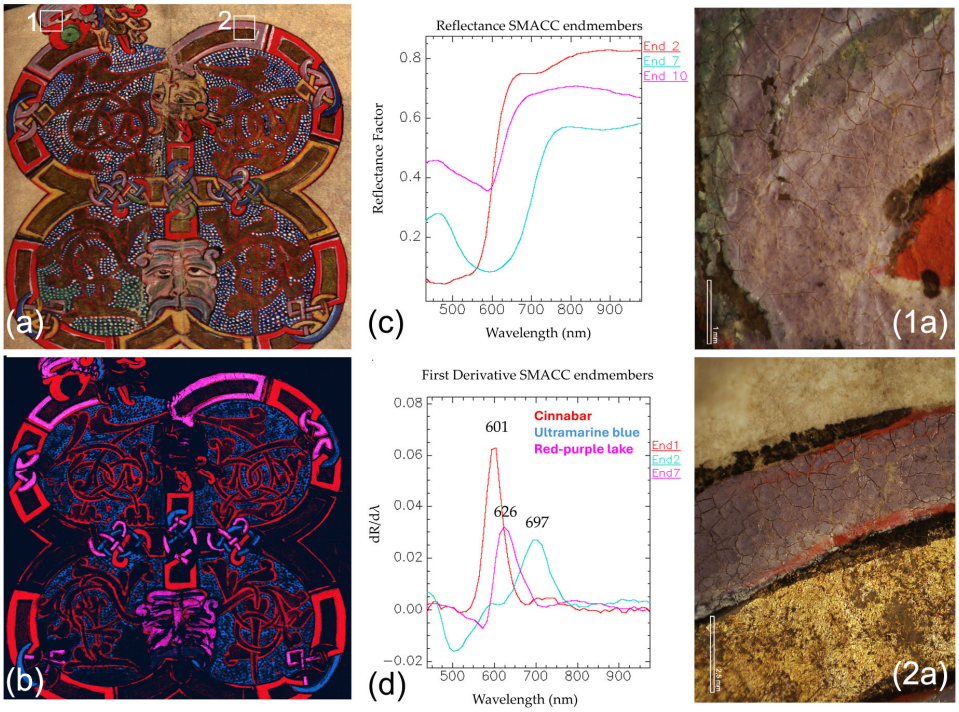

Figure 13. (**a**) RGB image of the folio 108r reconstructed from the 642 nm, 541 nm, and 460 nm bands of the hyperspectral datacube with white squares representing areas related to HRDM acquisitions (**1a**,**2a**); (**b**) SAM classification map; (**c**) endmembers extracted by SMACC routine performed on the reflectance cube for red, blue and purple pigment; (**d**) derivative endmember extracted. (**1a**,**2a**) HRDM images of areas 1 and 2, showing the purple hue and the proximity of cinnabar paints.

Gilding

The gilded areas characterised by XRF analysis, revealed Au as the dominant element (Figure 14), confirming the use of gold-based materials for the decoration. Minor amounts of Ag were also detected, which may reflect either the natural composition of gold or its intentional alloying with silver to modify colour and reduce material cost. The comparison between the spectra acquired at points 1 and 2 (Figure 14c) shows higher gold counts in

Point 1, whereas point 2 exhibits higher silver counts. This difference may indicate the intentional addition of silver to achieve a darker tonal variation, indicating the use of shell gold.

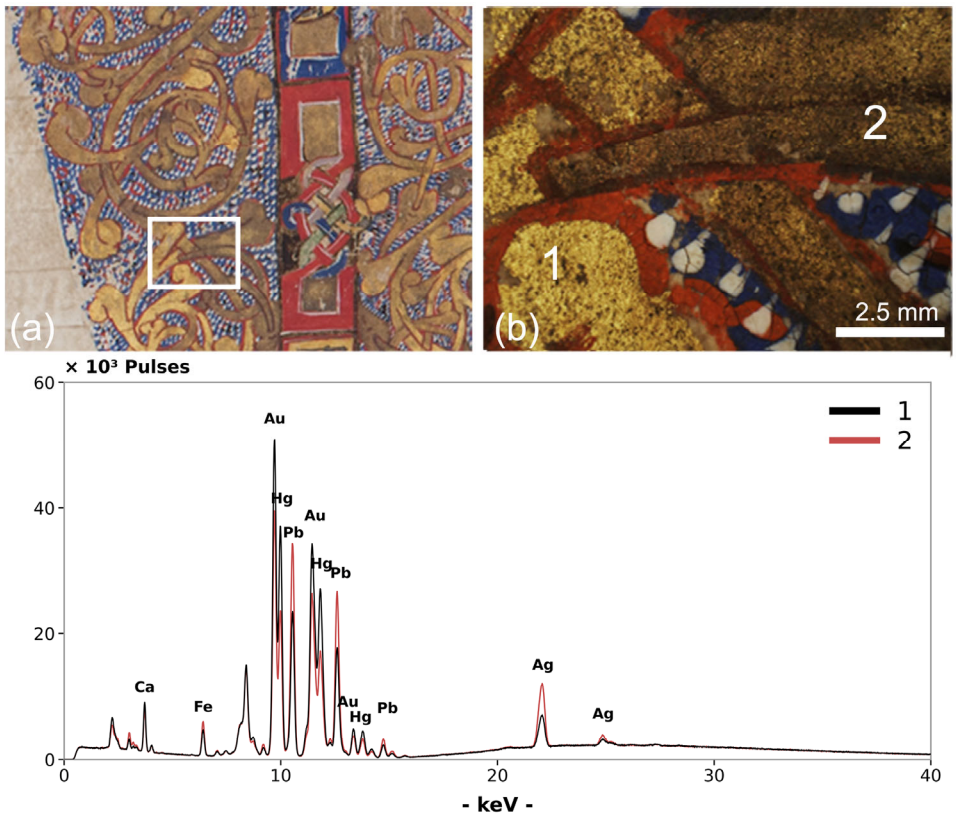

Figure 14. (**a**) Photograph of the gilded detail. The white square indicates the area selected for HRDM acquisition. (**b**) HRDM image of the selected area. (**c**) XRF spectra acquired at points 1 (black) and 2 (red) in (**b**).

4. Discussion

4.1. The Materials (Pigment, Binder, and Ink) Used in the Three Manuscripts (RQ1)

A first application of the integrated research protocol enables the comparative interpretation of analytical data from two Manuscript Production Environments (MPEs), represented here by the "Santorale" manuscripts (Mss. 7 and 17) and the "Messale–breviario" (Ms. 19). Across the three manuscripts, the principal pigments are comparable: cinnabar for red areas and rubrics; natural ultramarine for blue; lead white for white highlights and tonal adjustment, and copper-based compound for green. The identification of the copper-based green pigment in the examined manuscripts proved challenging, a well-documented difficulty for non-invasive approaches [49,58]. While a copper carbonate can be excluded by FTIR, the amorphous morphology is instead consistent with verdigris, a copper acetate compound widely employed in medieval manuscript illumination [57–60]. However, the spectroscopic complexity of verdigris in aged samples is a well-recognised phenomenon: copper acetates are known to dissolve over time within the binder, rendering them undetectable by reflection FTIR [49]. This degradation pathway is further complicated in proteinaceous media, where copper–protein interactions may suppress or shift the diagnostic carboxylate stretching bands [48,61]. In the manuscripts analysed, the detection of calcium/copper oxalates in the FTIR spectra is consistent with long-term degradation processes documented for copper-based green pigments, where oxalate formation has

been attributed to the reaction between the pigment and organic binders or environmental agents [49,60]. Alternatively, the pigment could belong to the broader category of medieval copper greens that, depending on the preparation recipe, may yield a mixture of copper acetate with oxalates or chloride-based compounds such as atacamite [60]. The corrosive nature of verdigris on parchment supports was moreover well known to medieval practitioners themselves, as documented in late 14th-century technical treatises such as De Arte Illuminandi, which mentions verdigris without providing a recipe precisely because of the potential damage it could cause to the support [48]. At present, both the verdigris hypothesis and the possibility of a more complex copper green formulation remain consistent with the available data.

The iron-gall ink employed for the written text was consistently identified across all three manuscripts, although the ongoing palaeographical analysis does not yet allow these practices to be associated with specific phases or discontinuities in the writing process. In addition, a brown ink, whose composition remains uncertain, was employed in preparatory underdrawings and yellowish decorative details. The use of iron-gall ink in Ms19 (G10) as a pictorial component is consistent with the findings of Aceto and Calà [28], whose systematic survey of Western illuminated manuscripts dating from the sixth to the sixteenth century demonstrated that iron-gall ink was widely employed not only as a writing and drawing medium but also as a colorant for figurative details, letter outlines, and preparatory sketches.

The large initials and the figurative inserts reveal a remarkable level of skill and full technical maturity in the use of colour, achieved both through the application of individual pigments and through refined mixtures designed to produce a wide range of chromatic gradations, with extensive and deliberate use of ink also for colourist purposes. The figure of Stephanus Sacerdos is, in many respects, emblematic of the illuminator's skill and technical mastery. Employing cinnabar and minium, sometimes blended, and enriching the palette with the addition of ultramarine blue, the illuminator renders the preciousness of the tunic and its minute decorations through sophisticated chromatic effects of remarkable quality. The same expertise is evident in the nuanced use of ultramarine blue to shade the forehead and mouth of the lower mask that adorns the monogram, alternating it with a copper-based green on a purple background, probably achieved using a lake dye. The predominant use of precious ultramarine blue—applied both in its pure form and, to a lesser extent, mixed with lead white—not only attests to the manuscript's exceptional value but also suggests a relatively ready availability of this pigment; a deeper exploration into procurement strategies and the circulation of this valuable material merits further investigation. The miniaturist also employs various copper-based shades of green, sometimes blending them with ink or dark pigments to achieve deeper tones, resulting in refined chromatic effects. It is worth noting that the admixture of orpiment with other components to obtain green hues is attested in medieval technical sources of direct relevance to the present context. The De coloribus et mixtionibus, a tradition already present in the *Mappae Clavicula* and in Theophilus, prescribes mixing orpiment with black to produce a green (gladus green), lightening or darkening the tone by adjusting the proportions of each component [62]. Similarly, the *Liber colorum secundum magistrum Bernardum* describes a green obtained by grinding orpiment with indigo and Arabic gum [63]. The detection of orpiment in admixture with other components in the green areas of Ms. 19 is therefore consistent with documented medieval practice. Notable differences between the two production environments emerge in the yellow and purple chromatic areas. In the Sanctorale (Ms. 7 and Ms. 17), the yellow pigment exhibits a reflectance spectrum more consistent with an organic yellow lake than with a mineral pigment. In contrast, orpiment (As_2S_3) was unambiguously identified as the yellow pigment in Ms. 19. The purple hue in Ms. 19 appears to be a distinct colorant

rather than a mixture of red and blue pigments; its spectral features are compatible with a red–purple lake pigment [39,55,56]. The absence of reflectance features diagnostic of madder or cochineal lake, combined with the chronological context of the manuscript, points towards brazilwood lake, orchil, or folium as the most plausible candidates. The use of minium represents a further point of divergence: within the analysed manuscripts, it appears exclusively in Ms. 19, in the depiction of the shoes and garment of Stephanus Sacerdos. The use of gold (with minor Ag content) is also restricted to Ms. 19, for gilding.

From the binder perspective, the available FTIR data suggest substantial similarities among the three manuscripts, with proteinaceous materials representing the dominant binding media and occasional indications of a lipidic component. In several areas, particularly those containing iron-gall ink, spectral features may also indicate the presence of Arabic gum, although proteinaceous and saccharide binders are not mutually exclusive. Binder identification by reflectance FTIR remains challenging due to the strong spectral contribution of parchment collagen and the overlap of Amide bands from different proteinaceous materials. Amide I band, for instance, commonly observed between 1660 and 1690 cm^{-1}, with shifts to lower wavenumbers in old parchments, making it sometimes unreliable for certain binder identification [64]. However, slight shifts in colored areas (compared to unpigmented parchment support), or in some cases (Ms 17) shoulder in the amide II band, allow for a possible discrimination of a proteinceous binder, such as egg white [43], which is known to be widely used for illuminated [65]. Accordingly, binder-related inferences are treated as provisional within the present MPE-level inventory and are best refined through expanded sampling and complementary observations.

4.2. Underdrawings as an Essay of the MPEs Workflow (RQ2)

High resolution image and hyperspectral mapping reveal the presence of preparatory underdrawings in the painted surfaces of the illuminated initials across all three manuscripts. A degree of morphological differentiation is observable between the two manuscripts: in Ms. 17, the preparatory lines appear more pronounced. These observations are consistent with well-documented practices in medieval manuscript illumination. Underdrawings range from rapidly executed sketches to highly finished compositions anticipating every detail of the final decoration, and were typically executed with a hard metal point, charcoal, or diluted ink [66]. The latter appears to be the case in the manuscripts investigated here, where the attenuated and often nearly transparent strokes are consistent with the use of ink diluted precisely to facilitate concealment beneath the overlying pigment layers. The practice was central to the collaborative organisation of manuscript production, where a master's drawing could be coloured by workshop assistants, or a single illuminator could both draw and paint an entire decorative cycle. Differences in underdrawing style and execution therefore offer valuable insights into the division of labour and the working methods of individual artists or workshops.

4.3. A Preliminary Inventory of Production and Conservation Markers (RQs3 and 4)

The production-related features discussed above provide a first material baseline for the manuscripts examined here. At this stage, the results do not yet constitute a complete repertory of materials, techniques, and operational relationships for the MPEs under consideration. They do, however, allow an initial set of markers to be outlined for organizing the evidence and supporting future comparison. Excluding paleographical markers, which fall outside the scope of the diagnostic investigations, these comprise material and ornamental markers, concerning pigments, binders, and inks; process-related markers, linked to execution sequences; and conservation markers, associated with pigment degradation hypotheses and residues of materials not directly related to production.

These markers are not intended to define the modus operandi of a production environment in isolation, but to provide a comparative baseline for assessing other contemporary productions. The differences observed between the diagnostic datasets of Ms. 19 and Ms. 7 show how such markers may begin to distinguish production contexts. Nevertheless, diagnostic evidence must be integrated with paleographical, codicological, and art-historical data in order to support group-level description and historically grounded attribution. The pigment repertory identified here therefore contributes to the more precise historical placement of these productions within their territorial frame of reference, while remaining provisional and open to refinement through further observations and additional campaigns on other manuscripts from the collection. The interpretation of the analytical results must therefore consider this conservation history and the associated material modifications. Among the degradation processes observed, chromatic alteration related to chemical transformations of copper-based pigments has been reported [51], together with loss of cohesion in the pictorial layer, particularly in copper-based green paints, associated with protein binder degradation and the formation of calcium oxalates [51]. These factors must therefore be considered when assessing tonal variation, pigment identification, and the interpretive scope of point-based analytical data. The history of conservation can be complemented by a reconstruction of the use history of the Beneventan codices, based on residual traces of materials unrelated to their production. Circular beeswax stain, identified by FT-IR analyses, are frequently observed on the manuscripts examined here, as well as across the wider collection. Such evidence may support diachronic lines of investigation, from mapping the density and distribution of the deposits across different codices to analysing any fossil microbiome potentially preserved within the wax [67]. While these data do not directly inform the reconstruction of manuscript production environments, they offer a promising basis for exploring the successive environments through which the manuscripts circulated over time.

5. Conclusions

The results of complementary non-invasive analyses provide valuable evidence for reconstructing the profiles of the craftsmen involved in making the manuscripts, in particular the illuminators. These data make it possible to integrate and expand the limited technical-executive and stylistic-formal observations hitherto based exclusively on autoptic analysis and primarily focused on Ms. 19. Although not comparable in terms of preciousness and craftsmanship, the decorations in Ms. 7 and Ms. 17 also reveal elements of particular interest, starting with the use of ultramarine blue even in the smaller initials. The anthropomorphic elements used in the terminals of the initials, painted in a cursive style, help to define their cultural context and confirm once again the use of ink as a pigment. Extending the investigation to other manuscripts in the same series would be of great interest to formulate a hypothesis regarding the probable distinction between the illuminators involved in the decoration of these codices, as suggested by certain technical and stylistic inconsistencies in the ornamentation. It would be equally important to carry out research on other contemporary manuscripts, starting with the second volume of the breviary-missal (Ms 20), currently undergoing restoration. This would enable us to broaden our knowledge base, providing new insights that would help reconstruct the artists' working methods, their techniques, and the materials they used.

Supplementary Materials: The following supporting information can be downloaded at: https://www.mdpi.com/article/10.3390/heritage9070280/s1. Figure S1–S7: Representative analytical results (FTIR, Raman, XRF, Vis-NIR Reflectance spectra) obtained from black letter, parchment, red, yellow, green, blue, white, pink/purple of Ms. 7, Ms. 17, and Ms. 19. Figure S8: Endmembers extracted by dog detail of Ms. 19. Figure S9: Reference reflectance spectra for red–purple lake

pigments. Table S1: Hyperspectral imaging acquisition parameters for each investigated folio. Section S1: Parchment Characterisation.

Author Contributions: Conceptualization, G.T.C. and F.D.C.; methodology, F.D.C., M.C., A.C.M., M.F. (Myriam Fiore) and M.G.; investigation, M.C., A.C.M., M.F. (Myriam Fiore) and M.G.; formal analysis, M.C., A.C.M., M.F. (Myriam Fiore), M.G. and M.F. (Myriam Fiore); resources, M.I.; data curation, A.C., M.C., M.F. (Marco Ferretti), A.C.M., M.F. (Myriam Fiore) and M.G.; writing—original draft preparation, F.D.C., A.C., A.C.M., M.F. (Myriam Fiore), M.G. and M.C.; writing—review and editing, C.M.; visualization, A.C.M. and M.G.; supervision, G.T.C.; project administration, G.T.C.; funding acquisition, C.M. All authors have read and agreed to the published version of the manuscript.

Funding: This research was funded by the project Patrimonio culturale e creatività nelle transizioni verde e digitale per società inclusive, funded by MUR under the FOE programme (CUP B63C21000940005). This work was also supported by E-RIHS.it, national node of the European Research Infrastructure for Heritage Science (financial support by MUR, Ministero dellUniversità e della Ricerca, FOE E-RIHS IT and PON Ricerca e Innovazione 2014-2020, CCI: 014IT16M2OP005). Additional support was provided by H2IOSC Project—Humanities and Cultural Heritage Italian Open Science Cloud funded by the European Union NextGenerationEU—National Recovery and Resilience Plan (NRRP)—Mission 4 "Education and Research" Component 2 "From research to business" Investment 3.1 "Fund for the realization of an integrated system of research and innovation infrastructures" Action 3.1.1 "Creation of new research infrastructures strengthening of existing ones and their networking for Scientific Excellence under Horizon Europe"—Project code IR0000029—CUP B63C22000730005.

Data Availability Statement: The original contributions presented in this study are included in the article. Further inquiries can be directed to the corresponding author.

Acknowledgments: The authors wish to thank the Cathedral Chapter Library of Benevento (Biblioteca Capitolare di Benevento) and its staff for granting access to the manuscripts and for their support during the analytical campaigns. This contribution is conducted within the National PhD project in Heritage Science (University la Sapienza of Rome): "Per una ricostruzione degli scriptoria della città di Benevento (VIII–XV secolo): produzione, memoria, ordinamento e tutela digitale".

Conflicts of Interest: The authors declare no conflicts of interest. The funders had no role in the design of the study; in the collection, analyses, or interpretation of data; in the writing of the manuscript; or in the decision to publish the results.

References

1. Di Benevento, F.; D'Angelo, E. (Eds.) *Chronicon Beneventanum: Città e Feudi Nell'Italia dei Normanni*; SISMEL Edizioni del Galluzzo: Firenze, Italy, 1998.
2. Martin, J.-M. *Chronicon Sanctae Sophiae; Fonti per la Storia Dell'Italia Medievale*; Istituto Storico Italiano per il Medio Evo: Rome, Italy, 2000.
3. Cuozzo, E.; Esposito, L.; Martin, J.-M. *Le Pergamene del Monastero di Santa Sofia di Benevento (762–1067)*; Sources et Documents 12/1; École française de Rome: Rome, Italy, 2021.
4. Vehse, O. *Benevent als Territorium des Kirchenstaates Bis zum Beginn der Avignonesischen Epoche*; QFIAB; German Historical Institute Rome: Rome, Italy, 1932; Volume 22, pp. 87–160.
5. Matera, V. Notai e Giudici a Benevento nei Secoli XI e XII. In *La Produzione Scritta Tecnica e Scientifica nel Medioevo: Libro e Documento tra Scuole e Professioni*; De Gregorio, G., Galante, M., Eds.; Fondazione Centro Italiano di Studi sull'Alto Medioevo: Spoleto, Italy, 2009.
6. Araldi, G. Trasformazioni sociali e istituzionali in una città pontificia del mezzogiorno d'Italia: Gli statuti di Benevento del 1203. In *Comparing Two Italies: Civic Tradition, Trade Networks, Family Relationships Between the Italy of Communes and the Kingdom of Sicily*; Mainoni, P., Barile, N.L., Eds.; Mediterranean Nexus 1100–1700; Brepols: Turnhout, Belgium, 2020.
7. Lowe, E.A.; Brown, V. *The Beneventan Script: A History of the South Italian Minuscule*, 2nd ed.; Edizioni di Storia e Letteratura: Rome, Italy, 1980.
8. Mallet, J.; Thibaut, A. *Les Manuscrits en Écriture Bénéventaine de la Bibliothèque Capitulaire de Bénévent*; Éditions du Centre National de la Recherche Scientifique: Paris, France, 1984; Volume 1.

9. Pietroni, E.; Chirivì, A.; Greco, M.; Pandurino, A.; Bucciero, A.; Lupinacci, A.; Aloisi, R.; Cozza, M. The Illuminated Manuscripts Pilot Project: A Hub Dedicated to the Interdisciplinary Study of Ancient Codices, Integrated into the DigiLab-IT Platform. In Proceedings of the Digital Heritage 2025, Siena, Italy, 8–13 September 2025. [CrossRef]
10. Chirivì, A.; Pietroni, E.; Greco, M.; Pandurino, A.; Bucciero, A. An Evolving Scenario in the Study of Illuminated Manuscripts: Innovative Approaches to Research Questions. *Digit. Appl. Archaeol. Cult. Herit.* **2026**, *40*, e00496. [CrossRef]
11. Campana, A. Per la storia della Biblioteca Capitolare di Benevento. *Bull. dell'Archivio Paleografico Ital. (Nuova Ser.)* **1956**, *2*, 141–167.
12. Iadanza, M. Note di descrizione dei Benev. 1 e Benev. 4 della Biblioteca Capitolare di Benevento. *Studi Beneventani* **1988**, *7*, 119–139.
13. Mallet, J.; Thibaut, A. *Les Manuscrits en Écriture Bénéventaine de la Bibliothèque Capitulaire de Bénévent*; Éditions du Centre National de la Recherche Scientifique: Paris, France, 1997; Volume 2.
14. Pertusi, A. La Contesa per le Reliquie di S. Nicola tra Bari, Venezia e Genova. *Quad. Mediev.* **1978**, *5*, 6–56.
15. Giordano, M. Il Martirologio VIII C 5 della Biblioteca Nazionale di Napoli e il problema della localizzazione del Monastero di Santa Maria del Plesco. *Riv. Terra Lav.* **2018**, *13*, 70–83.
16. De Duonni, V. Echi pugliesi nella produzione manoscritta di Montevergine tra XII e XIII secolo. In *Letteratura Erudita, Fonti e Documenti d'Archivio. Per una Storia di San Giovanni in Venere e del Mezzogiorno Adriatico*; Rossi, M.C., De Duonni, V., Madonna, M.A., Eds.; Volturnia edizioni: Cerro al Volturno, Italy, 2020; pp. 213–225.
17. Elba, E. Lungo le rotte adriatiche: Il Libro d'ore in beneventana di Budapest e la miniatura pugliese dell'XI secolo. *Riv. Stor. Miniatura* **2008**, *12*, 45–55.
18. Biblioteca Apostolica Vaticana. Vat. lat. 4939. Available online: https://digi.vatlib.it/view/MSS_Vat.lat.4939 (accessed on 6 May 2026).
19. Biblioteca Apostolica Vaticana. Vat. lat. 4928. Available online: https://digi.vatlib.it/view/MSS_Vat.lat.4928 (accessed on 6 May 2026).
20. Brenk, B. Roma Biblioteca Casanatense, cas. 724 (B I 13) 3, Exultet. In *Exultet: Rotoli Liturgici del Medioevo Meridionale*; Cavallo, G., Director; Orofino, G., Pacere, O., Coordinator; Istituto poligrafico dello Stato: Rome, Italy, 1994; pp. 319–339.
21. Porter, C. Laser Raman Spectroscopy—A Tool for Non-Destructive Pigment Analysis of Manuscripts. *Pap. Conserv.* **1992**, *16*, 93–97. [CrossRef]
22. Burgio, L.; Clark, R.J.H. Library of FT-Raman Spectra of Pigments, Minerals, Pigment Media and Varnishes, and Supplement to Existing Library of Raman Spectra of Pigments with Visible Excitation. *Spectrochim. Acta Part A Mol. Biomol. Spectrosc.* **2001**, *57*, 1491–1521. [CrossRef]
23. Caggiani, M.C.; Colomban, P. Raman Microspectroscopy for Cultural Heritage Studies. *Phys. Sci. Rev.* **2018**, *3*, 20180007. [CrossRef]
24. Green, A.A.; Berman, M.; Switzer, P.; Craig, M.D. A Transformation for Ordering Multispectral Data in Terms of Image Quality with Implications for Noise Removal. *IEEE Trans. Geosci. Remote Sens.* **1988**, *26*, 65–74. [CrossRef]
25. Gruninger, J.H.; Ratkowski, A.J.; Hoke, M.L. The Sequential Maximum Angle Convex Cone (SMACC) Endmember Model. In *Algorithms and Technologies for Multispectral, Hyperspectral, and Ultraspectral Imagery X*; SPIE: Bellingham, WA, USA, 2004; Volume 5425.
26. Kruse, F.A.; Lefkoff, A.B.; Boardman, J.W.; Heidebrecht, K.B.; Shapiro, A.T.; Barloon, P.J.; Goetz, A.F.H. The Spectral Image Processing System (SIPS)—Interactive Visualization and Analysis of Imaging Spectrometer Data. *Remote Sens. Environ.* **1993**, *44*, 145–163. [CrossRef]
27. Delaney, J.K.; Dooley, K.A.; Radpour, R.; Kakoulli, I. Macroscale Multimodal Imaging Reveals Ancient Painting Production Technology and the Vogue in Greco-Roman Egypt. *Sci. Rep.* **2017**, *7*, 15509. [CrossRef] [PubMed]
28. Aceto, M.; Calà, E. Analytical Evidences of the Use of Iron-Gall Ink as a Pigment on Miniature Paintings. *Spectrochim. Acta Part A Mol. Biomol. Spectrosc.* **2017**, *187*, 1–8. [CrossRef]
29. Retko, K.; Legan, L.; Kosel, J.; Ropret, P. Identification of Iron Gall Inks, Logwood Inks, and Their Mixtures Using Raman Spectroscopy, Supplemented by Reflection and Transmission Infrared Spectroscopy. *Herit. Sci.* **2024**, *12*, 212. [CrossRef]
30. Bicchieri, M.; Monti, M.; Piantanida, G.; Sodo, A. Non-Destructive Spectroscopic Investigation on Historic Yemenite Scriptorial Fragments: Evidence of Different Degradation and Recipes for Iron Tannic Inks. *Anal. Bioanal. Chem.* **2013**, *405*, 2713–2721. [CrossRef] [PubMed]
31. Derkacheva, O.Y.; Neelova, A.D.; Bystrova, E.S. Identification of Inks in 15th Century Paper Manuscripts Using Micro-Raman Spectroscopy. *Nanobiotechnol. Rep.* **2025**, *20*, 581–589. [CrossRef]
32. Caterino, S.; Caniola, I.M.; Pignitter, M.; Zoleo, A.; Crestini, C.; Sanchez-Cortés, S.; Cappa, F. A Systematic Multianalytical Approach in the Study of Iron–Polyphenolic Complexes in Iron-Gall Inks. *Inorg. Chem.* **2025**, *64*, 4802–4816. [CrossRef] [PubMed]
33. Lee, A.S.; Mahon, P.J.; Creagh, D.C. Raman Analysis of Iron Gall Inks on Parchment. *Vib. Spectrosc.* **2006**, *41*, 170–175. [CrossRef]
34. Rosi, F.; Daveri, A.; Miliani, C.; Verri, G.; Benedetti, P.; Piqué, F.; Brunetti, B.G.; Sgamellotti, A. On the Use of Overtone and Combination Bands for the Analysis of the $CaSO_4$–H_2O System by Mid-Infrared Reflection Spectroscopy. *Appl. Spectrosc.* **2010**, *64*, 956–963. [CrossRef] [PubMed]

35. Nodari, L.; Ricciardi, P. Non-Invasive Identification of Paint Binders in Illuminated Manuscripts by ER-FTIR Spectroscopy: A Systematic Study of the Influence of Different Pigments on the Binders' Characteristic Spectral Features. *Herit. Sci.* **2019**, *7*, 7. [CrossRef]
36. Longoni, M.; Miliani, C.; Rosi, F.; Brunetti, B.G.; Sgamellotti, A. Near-Infrared Combination Bands of Parchment as Tools for Conservation Assessment. In Proceedings of the 9th International Conference on NDT of Art, Jerusalem, Israel, 25–30 May 2008.
37. Buckley, M.; Whitcher Kansa, S.; Howard, S.; Campbell, S.; Thomas-Oates, J.; Collins, M. Distinguishing between Archaeological Sheep and Goat Bones Using a Single Collagen Peptide. *J. Archaeol. Sci.* **2010**, *37*, 13–20. [CrossRef]
38. Volpi, F.; Neri, P.; Pranzini, G. Parchment: Structure, Degradation and Conservation. In *Handbook of Archaeological Sciences*; Brothwell, D.R., Pollard, A.M., Eds.; Wiley: Chichester, UK, 2001; pp. 679–685.
39. Aceto, M.; Agostino, A.; Fenoglio, G.; Idone, A.; Gulmini, M.; Picollo, M.; Ricciardi, P.; Delaney, J.K. Characterisation of Colourants on Illuminated Manuscripts by Portable Fibre Optic UV-Visible-NIR Reflectance Spectrophotometry. *Anal. Methods* **2014**, *6*, 1488–1500. [CrossRef]
40. Burgio, L.; Clark, R.J.H.; Muralha, V.S.; Stanley, T. Pigment Analysis by Raman Microscopy of the Non-Figurative Illumination in 16th- to 18th-Century Islamic Manuscripts. *J. Raman Spectrosc.* **2008**, *39*, 1482–1493. [CrossRef]
41. Monico, L.; Rosi, F.; Miliani, C.; Daveri, A.; Brunetti, B.G. Non-Invasive Identification of Metal-Oxalate Complexes on Polychrome Artwork Surfaces by Reflection Mid-Infrared Spectroscopy. *Spectrochim. Acta Part A Mol. Biomol. Spectrosc.* **2013**, *116*, 270–280. [CrossRef]
42. Zoleo, A.; Nodari, L.; Rampazzo, M.; Piccinelli, F.; Russo, U.; Federici, C.; Brustolon, M. Characterization of Pigment and Binder in Badly Conserved Illuminations of a 15th-Century Manuscript. *Archaeometry* **2014**, *56*, 496–512.
43. Zaffino, C.; Guglielmi, V.; Faraone, S.; Vinaccia, A.; Bruni, S. Exploiting External Reflection FTIR Spectroscopy for the In-Situ Identification of Pigments and Binders in Illuminated Manuscripts. Brochantite and Posnjakite as a Case Study. *Spectrochim. Acta Part A Mol. Biomol. Spectrosc.* **2015**, *136*, 1076–1085. [CrossRef]
44. Schmidt, C.M.; Walton, M.S.; Trentelman, K. Characterization of Lapis Lazuli Pigments Using a Multitechnique Analytical Approach. *Anal. Chem.* **2009**, *81*, 8513–8518. [CrossRef] [PubMed]
45. Innocenti, S.; Quintero Balbas, D.; Galeotti, M.; Cagnini, A.; Porcinai, S.; Striova, J. Historical Pigments and Paint Layers: Raman Spectral Library with 852 nm Excitation Laser. *Minerals* **2024**, *14*, 557. [CrossRef]
46. Miliani, C.; Daveri, A.; Brunetti, B.G.; Sgamellotti, A. CO2 Entrapment in Natural Ultramarine Blue. *Chem. Phys. Lett.* **2008**, *466*, 148–151. [CrossRef]
47. Cucci, C.; Delaney, J.K.; Picollo, M. Reflectance Hyperspectral Imaging for Investigation of Works of Art: Old Master Paintings and Illuminated Manuscripts. *Acc. Chem. Res.* **2016**, *49*, 2070–2079. [CrossRef] [PubMed]
48. Miliani, C.; Rosi, F.; Daveri, A.; Brunetti, B.G. Reflection Infrared Spectroscopy for the Non-Invasive In Situ Study of Artists' Pigments. *Appl. Phys. A* **2012**, *106*, 295–307.
49. Buti, D.; Rosi, F.; Brunetti, B.G.; Miliani, C. In-Situ Identification of Copper-Based Green Pigments on Paintings and Manuscripts by Reflection FTIR. *Anal. Bioanal. Chem.* **2013**, *405*, 2699–2711. [CrossRef] [PubMed]
50. Hernández, B.; Pflüger, F.; Kruglik, S.G.; Ghomi, M. Characteristic Raman Lines of Phenylalanine Analyzed by a Multiconformational Approach. *J. Raman Spectrosc.* **2013**, *44*, 827–833. [CrossRef]
51. Melo, M.J.; Araújo, R.; Castro, R.; Casanova, C. Colour Degradation in Medieval Manuscripts. *Microchem. J.* **2016**, *124*, 837–844. [CrossRef]
52. Guerra, M.; Manso, M.; Pessanha, S.; Le Gac, A.; Longelin, S.; Guilherme, A.; Carvalho, M.L. X-Ray Fluorescence Spectrometry as a Diagnostic Tool in Characterization and Conservation of Manueline Illuminated Manuscripts. In *Cultural Heritage: Protection, Developments and International Perspectives*; Nova Science Publishers: New York, NY, USA, 2013; pp. 235–256.
53. Miliani, C.; Daveri, A.; Spaabaek, L.; Romani, A.; Manuali, V.; Sgamellotti, A.; Brunetti, B.G. Bleaching of Red Lake Paints in Encaustic Mummy Portraits. *Appl. Phys. A* **2010**, *100*, 703–711. [CrossRef]
54. Longoni, M.; Genova, B.; Marzanni, A.; Melfi, D.; Beccaria, C.; Bruni, S. FT-NIR Spectroscopy for the Non-Invasive Study of Binders and Multi-Layered Structures in Ancient Paintings: Artworks of the Lombard Renaissance as Case Studies. *Sensors* **2022**, *22*, 2052. [CrossRef] [PubMed]
55. Monico, L.; Prati, S.; Sciutto, G.; Catelli, E.; Romani, A.; Quintero Balbas, D.; Li, Z.; De Meyer, S.; Nuyts, G.; Janssens, K.; et al. Development of a Multi-Method Analytical Approach Based on the Combination of Synchrotron Radiation X-Ray Micro-Analytical Techniques and Vibrational Micro-Spectroscopy Methods to Unveil the Causes and Mechanism of Darkening of "Fake-Gilded" Decorations in a Cimabue Painting. *J. Anal. At. Spectrom.* **2022**, *37*, 114–129. [CrossRef]
56. Peruzzi, G.; Cosentino, A.; Aceto, M.; Miliani, C. Non-Invasive Identification of Dyed Textiles by Using VIS-NIR FORS and Hyperspectral Imaging Techniques. *Color Cult. Sci. J.* **2021**, *13*, 61–69. [CrossRef]
57. Roy, A.; Ashok, R.; Berrie, B.; Eastaugh, N. *Artists' Pigments: A Handbook of Their History and Characteristics*; Butterworth-Heinemann: Oxford, UK, 1993; Volume 1134.

58. Ricciardi, P.; Pallipurath, A.; Rose, K. 'It's Not Easy Being Green': A Spectroscopic Study of Green Pigments Used in Illuminated Manuscripts. *Anal. Methods* **2013**, *5*, 3819–3824. [CrossRef]
59. Scott, D.A.; Khandekar, N.; Schilling, M.R.; Turner, N. Technical Examination of a Fifteenth-Century German Illuminated Manuscript on Paper: A Case Study in the Identification of Materials. *Stud. Conserv.* **2001**, *46*, 93–108. [CrossRef]
60. Buse, B.; Otero, V.; Melo, M.J. New Insights into Synthetic Copper Greens: The Search for Specific Signatures by Raman and Infrared Spectroscopy for Their Characterization in Medieval Artworks. *Heritage* **2019**, *2*, 1255–1278. [CrossRef]
61. Zoleo, A.; Balliana, E.; Zendri, E.; Vigato, P.A. EPR and Spectroscopic Study of Naturally and Artificially Aged Copper Proteinate Compounds. *Spectrochim. Acta Part A Mol. Biomol. Spectrosc.* **2014**, *120*, 607–615.
62. Travaglio, P.; D'Olmo, P.B. De Coloribus et Mixtionibus: Tradition and Transmission of the Most Widespread Text on Mediaeval Illumination. *Medioev. Eur.* **2021**, *5*, 137–190.
63. Travaglio, P. Il 'Liber Colorum Secundum Magistrum Bernardum': Un trattato duecentesco di miniatura. *Studi Memofonte* **2016**, *16*, 149–195.
64. Vetter, W.; Latini, I.; Schreiner, M. Azurite in Medieval Illuminated Manuscripts: A Reflection-FTIR Study Concerning the Characterization of Binding Media. *Herit. Sci.* **2019**, *7*, 21. [CrossRef] [PubMed]
65. Van der Werf, I.D.; Calvano, C.D.; Germinario, G.; Cataldi, T.R.I.; Sabbatini, L. Chemical Characterization of Medieval Illuminated Parchment Scrolls. *Microchem. J.* **2017**, *134*, 146–153. [CrossRef]
66. Fitzwilliam Museum. MINIARE Project. Manuscripts and Their Making in the Renaissance. Available online: https://fitzmuseum.cam.ac.uk/research/projects/miniare (accessed on 6 May 2026).
67. Pavlović, J.; Sclocchi, M.C.; Planý, M.; Ruggiero, D.; Puškárová, A.; Bučková, M.; Šoltys, K.; Colaizzi, P.; Riccardi, M.L.; Pangallo, D.; et al. The Microbiome of Candle Beeswax Drops on Ancient Manuscripts. *Int. Biodeterior. Biodegrad.* **2022**, *174*, 105482. [CrossRef]

Disclaimer/Publisher's Note: The statements, opinions and data contained in all publications are solely those of the individual author(s) and contributor(s) and not of MDPI and/or the editor(s). MDPI and/or the editor(s) disclaim responsibility for any injury to people or property resulting from any ideas, methods, instructions or products referred to in the content.